THE FIBRES OF THE SCOTT MAP ON POLYGON TILINGS ARE THE FLIP EQUIVALENCE CLASSES

KARIN BAUR* AND PAUL P. MARTIN**

Abstract. We define a map from tilings of surfaces with marked points to strand diagrams, generalising Scott's construction for the case of triangulations of polygons. We thus obtain a map from tilings of surfaces to permutations of the marked points on boundary components, the *Scott map*. In the disk case (polygon tilings) we prove that the fibres of the Scott map are the flip equivalence classes.

The result allows us to consider the size of the image as a generalisation of a classical combinatorial problem. We hence determine the size in low ranks.

1. Introduction

In a groundbreaking paper [29] Scott proves that the homogeneous coordinate ring of a Grassmannian has a cluster algebra structure. In the process Scott gives a construction for Postnikov diagrams [25] starting from triangular tilings of polygons. Given a triangulation T, one decorates each triangle with 'strands'

The resultant strand diagram $\overrightarrow{\boldsymbol{\sigma}}(T)$ varies depending on the tiling, but induces a permutation $\boldsymbol{\sigma}(T)$ on the polygon vertex set that is the same permutation in each case. This construction is amenable to generalisation in a number of ways. For example, starting with the notion of triangulation for an arbitrary marked surface S [10, 11] (the polygon case extended to include handles, multiple boundary components, and interior vertices) there is a simplicial complex $A(S)$ of tilings [13, 14, 15] of which the triangulations are the top dimensional simplices. Lower simplices/tilings are obtained by deleting edges from a triangulation. There is a strand diagram $\overrightarrow{\boldsymbol{\sigma}}(T)$ in each case (we define it below, see Figure 1(a,b) for the heuristic). Thus each marked surface induces a subset $\boldsymbol{\sigma}(A(S))$ of the set of permutations of its boundary vertices (see Figures 2, 5 for examples).

This construction gives rise to a number of questions. The one we address here is, what are the fibres of this Scott map $\boldsymbol{\sigma}$. To give an intrinsic characterisation is a difficult problem in general. Here we give the answer in the polygon case, i.e. generalising $\boldsymbol{\sigma}(T)$, with fibre the set of all triangulations of the polygon, to the full A-complex of the polygon.

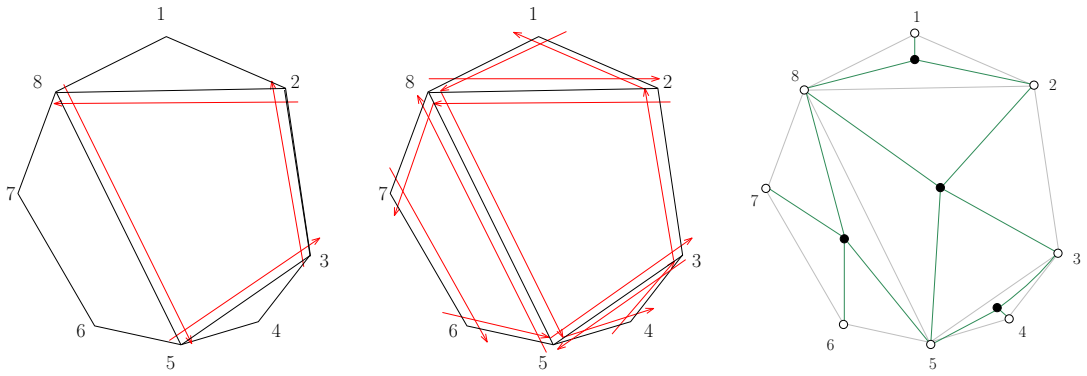

FIGURE 1. (a) Tile with strand segments; (b) tiling with strands; (c) induced plabic graph.

The answer is in terms of another crucial geometrical device used in the theory of cluster mutations [11] and widely elsewhere (see e.g. [14, 10, 16, 1] and cf. [9]) — flip equivalence (or the *Whitehead move*):

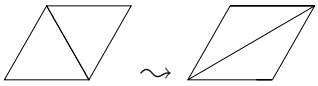

Our main Theorem, Theorem 2.1, can now be stated informally as in the title.

We shall conclude this introduction with some further remarks about related work. Then from §2 - §6 we turn to the precise definitions, formal statement and proof of Thm.2.1.

In §7 we report on combinatorial aspects of the problem — specifically the size of the image of the map $\boldsymbol{\sigma}$ in the polygon cases. The number of triangulations of polygons is given by the Catalan numbers. Taking the set A_r of all tilings of the r-gon, we have the little Schröder numbers (see e.g. [30, Ch.6]) The image-side problem is open. We use solutions to Schröder's problem and related problems posed by Cayley (as in [27, 24]), and our Theorem to compute the sequence in low rank r, and in §7.4 prove a key Lemma towards the general problem. To give a flavour of the set $\boldsymbol{\sigma}(A_r) \subset \Sigma_r$, the set of vertex permutations:

$$|\boldsymbol{\sigma}(A_r)| = 1, 2, 7, 26, 100, 404, 1691, \ldots \qquad (r = 3, 4, 5, \ldots, 9)$$

Finally in §8 we give some elementary applications of Theorem 2.1 to Postnikov's alternating strand diagrams and the closely related reduced plabic graphs [25]. In particular we consider a direct map G from tilings to plabic graphs generalising [26, §2]. (A heuristic for this 'stellar-replacement' map is given by the examples

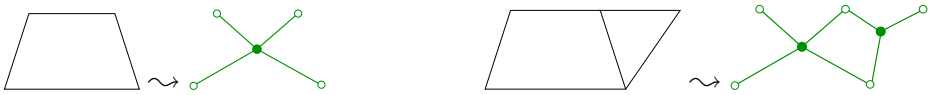

and then Figure 1(c).)

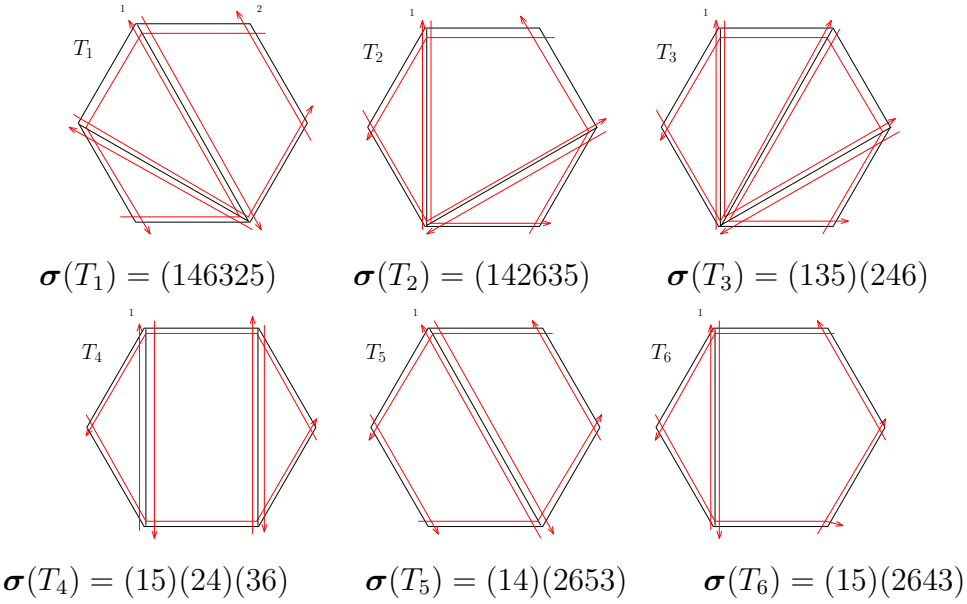

FIGURE 2. Examples of tilings, their strand diagrams and permutations

The geometry and topology of the plane, and of two-manifolds, continues to reward study from several perspectives. Recent motivations include modelling of anyons for Topological Quantum Computation [18], fusion categories [1], cluster categories [2, 8], Teichmüller spaces [10, 15], frieze patterns [5], diagram algebras [28, 17, 21], classical problems in combinatorics [20, 27] and combinatorics of symmetric groups and permutations [28]. In [2] Baur et al. used Scott's map [29] to produce strand diagrams for triangulated surfaces, again with the same permutation, in each case. This raises the intriguing question of which permutations are accessible in this way, and the role of the geometry in such constructions. Strictly speaking, the precise identification of permutations is dependent, in this setup, on a labelling convention. It is the numbers of permutations and the fibres over them (as we investigate here) that are, therefore, the main invariants accessible in the present formalism.

2. Definitions and results

Given any manifold X we write ∂X for the boundary and (X) for $X \setminus \partial X$. For a subset $D \in X$ we write $\overline{D}$ for its closure [22].

A *marked surface* is an oriented 2-manifold embedded in Euclidean 3-space, S; and a finite subset M. Set $M_\partial = M \cap \partial S$. An *arc* in marked surface (S, M) is a curve α in S such that (α) is an embedding of the open interval in $(S) \setminus M$; $\partial\alpha \subseteq M$; and if α cuts out a simple disk D from S then $|M \cap \overline{D}| > 2$.

Two arcs α, β in (S, M) are *compatible* if there exist representatives α' and β' in their isotopy classes such that $(\alpha') \cap (\beta') = \varnothing$.

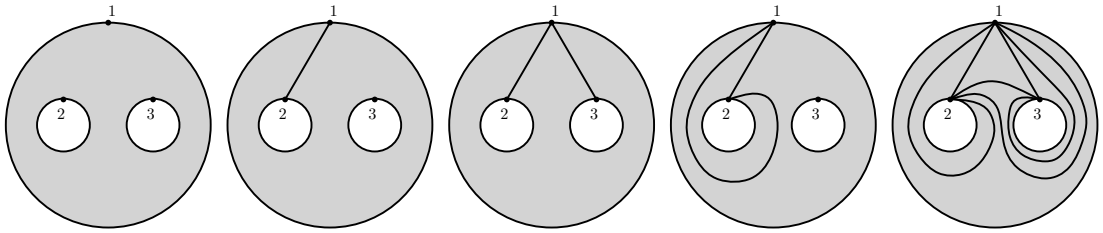

FIGURE 3. Tilings of the pants surface. Here $\kappa(S,M) = 6 \times 0 + 3 \times 3 + 2 \times 0 + 3 - 6 = 6$.

A *concrete tiling* of (S, M) is a collection of pairwise compatible arcs that are in fact pairwise non-intersecting. A *tiling* T is a boundary-fixing ambient isotopy class of concrete tilings — which we may specify by a concrete representative, with arc set $E(T)$ (it will be clear that this makes sense on classes). A *tile* of tiling T is a connected component of $S \setminus \cup_{\alpha \in E(T)} \alpha$. We write $F(T)$ for the set of tiles. (Note that if S is not homeomorphic to a disk then a tile need not be homeomorphic to a disk. For example a tile could be the whole of S in the case of Figure 3.)

Fixing (S, M), it is a theorem that there are maximal sets of compatible arcs. Set $\kappa(S, M) = 6g + 3b + 2p + |M| - 6$, where g is the genus, b the number of connected components of ∂S, and $p = |M \cap (S)|$. Suppose $\kappa(S, M) \geq 1$ and every boundary component intersects M. Then T maximal has $|E(T)| = \kappa(S, M)$, and every tile is a simple disk bounded by three arcs. Evidently given a tiling T then the removal of an arc yields another tiling. In this sense the set of tilings of (S, M) forms a simplicial complex, denoted $A(S, M)$.

We say two tilings are related by 'flip' if they differ only by the position of a diagonal triangulating a quadrilateral. The transitive closure of this relation is called *flip equivalence*. We write $[T]_\Delta$ for the equivalence class of the tiling T; and $Æ(S, M)$ for the set of classes of $A(S, M)$.

2.1. **The Scott map.** Let L be a connected component of the boundary of an oriented 2-manifold, and P a finite subset labeled $p_1, p_2, \ldots, p_{|P|}$ in the clockwise order (a traveller along P in the clockwise direction keeps the manifold on her right). Then an *umbral set* $P^\pm$ is a further subset of points p_i^- and p_i^+ $(i \in 1, 2, \ldots, |P|)$ such that the clockwise order of all these points is $\ldots, p_i, p_i^+, p_{i+1}^-, p_{i+1}, \ldots$. That is, the interval $(p_i^-, p_i^+) \subset L$ contains only p_i.

Given (S, M), let $M^\pm$ denote a fixed collection of umbral sets over all boundary components. A *Jordan diagram* d on (S, M) is a finite number of closed oriented curves in S together with a collection of $n = |M_\partial|$ oriented curves in S such that each curve passes from some p_i^+ to some p_j^- in $M^\pm$; and the collection of endpoints is $M^\pm$. Intersections of curves are allowed, but must be transversal. Write $\tau(d)$ for the permutation of M_∂ this induces. That is, if p_i^+ goes to p_j^- in d then $\tau(d)(i) = j$.

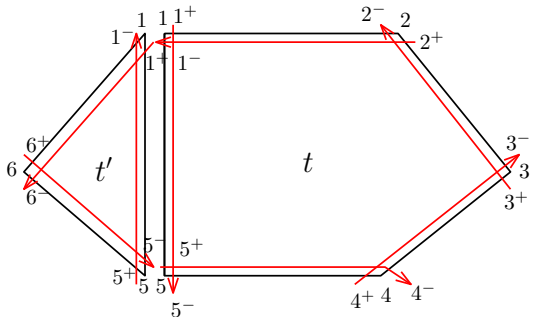

FIGURE 4. Composing tiles and strand segments. Here $\tau(d)(2) = 6$.

Diagram d is considered up to boundary-fixing isotopy. Let $\mathrm{Pu}(S, M)$ denote the set of Jordan diagrams.

Next we define a map $\overrightarrow{\boldsymbol{\sigma}} : A(S, M) \to \mathrm{Pu}(S, M)$. Consider a tiling T in $A(S, M)$. By construction each boundary L of a tile t is made up of segments of arcs, terminating at a set of points P. Hence we can associate $P^{\pm}$ to P as above. To arc segment s passing from p_i to p_{i+1} say, we associate a *strand segment* α_s in t passing from p_{i+1}^+ to p_i^-, such that the part of the tile on the s side of strand segment α_s is a topological disk. Finally strand segment crossings are transversal and minimal in number. See tile t in Figure 4 for example.

It will be clear that if two tiles meet at an arc segment then the umbral point constructions from each tile can be chosen to agree: as in Figure 4. Applying the α_s construction to every segment s of every tile t in T, we thus obtain a collection $\overrightarrow{\boldsymbol{\sigma}}(T)$ of strand segments in S forming strands whose collection of terminal points are at the umbral points of ∂S; so that $\overrightarrow{\boldsymbol{\sigma}}(T) \in \mathrm{Pu}(S, M)$. Altogether, writing Σ_M for the set of permutations of set M, we have $\boldsymbol{\sigma} : A(S, M) \to \Sigma_{M_\partial}$ defined by

$$\boldsymbol{\sigma} = \tau \circ \overrightarrow{\boldsymbol{\sigma}} \tag{1}$$

We call this the *Scott map*. It agrees with Scott's construction [29] in the case of triangulations of simple polygons.

We remark that the intermediate map $\overrightarrow{\boldsymbol{\sigma}}$ is injective, as we will show later (Theorem 8.4). The map $\boldsymbol{\sigma}$ however is clearly not injective, as the image of any triangulation of a polygon is the permutation induced by $i \mapsto i + 2$.

The focus of this article is the case where (S, M) is a polygon P with n vertices. We write A_n for $A(S, M)$ in this case, $Æ_n$ for $Æ(S, M)$, and Pu_n for $\mathrm{Pu}(S, M)$. Our main result can now be stated:

Theorem 2.1. *Let $T_1, T_2 \in A_n$ be tilings of an n-gon P. Then $\boldsymbol{\sigma}(T_1) = \boldsymbol{\sigma}(T_2)$ if and only if $[T_1]_\Delta = [T_2]_\Delta$.*

Sections 3, 4 and 5, 6 are concerned with the proof of this result.

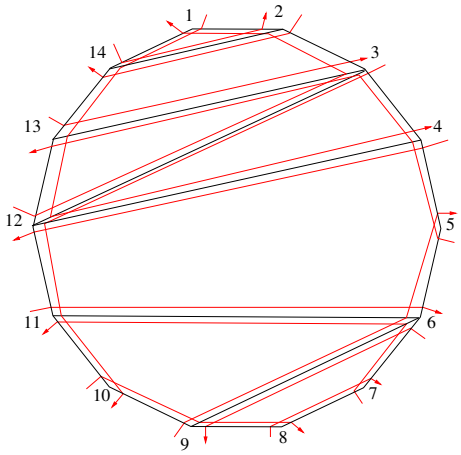

$\overset{\sigma}{\mapsto}$ (1,4, 12)(2, 14)(3,10,8,7,11,6,9,5,13)

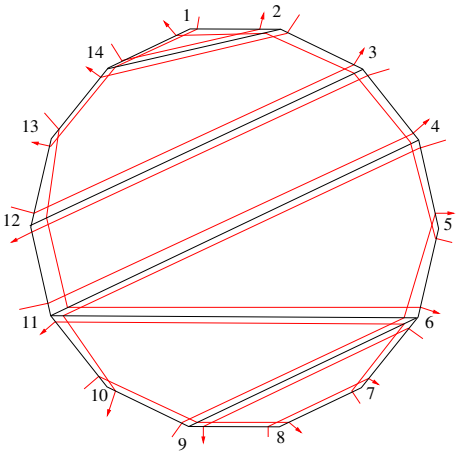

$\overset{\sigma}{\mapsto}$ (1,13,6,9,5)(2,14)(3,12)(4,10,8,7,11)

FIGURE 5. Examples of tilings, strands and Scott maps

We will see in Lemma 3.5 that $\overrightarrow{\boldsymbol{\sigma}}(A_n)$ lies in the subset of Pu_n of alternating strand diagrams [25, §14]. Theorem 2.1 is thus related to Postnikov's result [25, Corollary 14.2] that the permutations arising from two alternating strand diagrams are the same if and only if the strand diagrams can be obtained from each other through a sequence of certain kinds of 'moves'. Consider the effect of a flip on the associated strands:

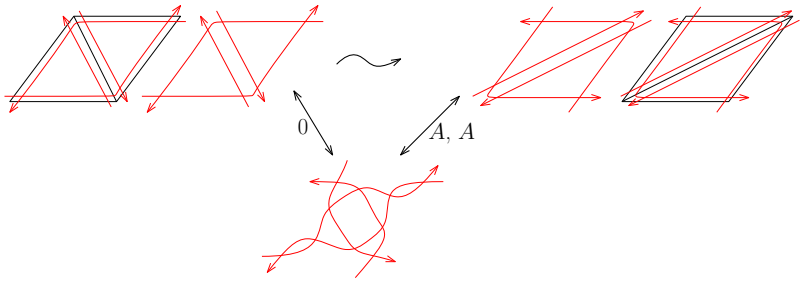

Comparing with Figure 14.2 of [25], the diagram shows that the flip corresponds to a certain combination of two types of Postnikov's three moves (see Figure 18).

2.2. **Notation for tilings of polygons.** We note here simplifying features of the polygon case that are useful in proofs.

Geometrically we may consider a tile as a subset of polygon P considered as a subset of $\mathbb{R}^2$. This facilitates the following definition.

Definition 2.2. Let $T \in A_n$. By $\mathrm{Tr}(T) \subset \mathbb{R}^2$ we denote the union of all triangles in T. We call T_1 and T_2 *triangulated-part equivalent* if $\mathrm{Tr}(T_1) = \mathrm{Tr}(T_2)$ and they agree on the complement of $\mathrm{Tr}(T_1)$. See Figure 6.

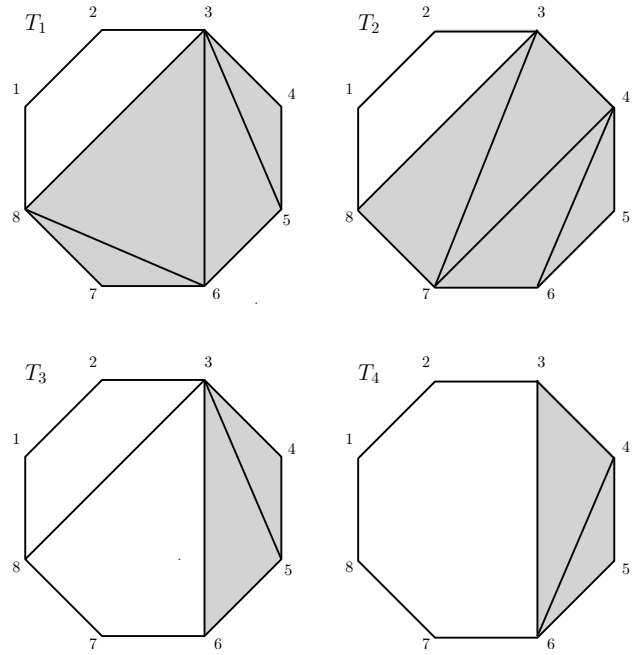

FIGURE 6. Tilings of an octagon, and the associated $\mathrm{Tr}(T_i)$. Note that T_1, T_2 are triangulated-part equivalent, but T_3, T_4 are not.

By Hatcher's Corollary in [14], two tilings are flip equivalent if and only if they are triangulated-part equivalent. The following is immediate.

Lemma 2.3. *Let T_1 and T_2 be tilings of an n-gon P. All tiles of size ≥ 4 agree in these tilings if and only if $[T_1]_\Delta = [T_2]_\Delta$.*

Write $\underline{n} = \{1, 2, \ldots, n\}$ for the vertex set of P, assigned to vertices as for example in Figure 5. The 'vertices' of A_n *as a simplicial complex* are the $n(n-3)/2$ diagonals. A diagonal between polygon vertices i, j is uniquely determined by the vertices. We write $[i, j]$ for such a diagonal. Here order is unimportant. A tiling in A_n can then be given as its set of diagonals. Example: The tiling from A_8 in Figure 1 is $T = \{[2, 8], [3, 5], [5, 8]\}$. An example of a top-dimensional simplex (triangulation) in A_8 of which this T is a face is $T \cup \{[3, 8], [6, 8]\}$.

Equally usefully, focussing instead on tiles, we may represent a tiling $T \in A_n$ as a subset of the power set $\mathcal{P}(\underline{n})$: for $T \in \mathcal{P}(\underline{n})$ one includes the subsets that are the vertex sets of tiles in T.

Example 2.4. In tile notation the tiling from A_8 in Figure 1 becomes

$$T = \{\{1, 2, 8\}, \{2, 3, 5, 8\}, \{3, 4, 5\}, \{5, 6, 7, 8\}\}$$

In this representation, while $A_2 = \varnothing$, and $A_3 = \{\{\{1, 2, 3\}\}\}$, we have:

$$A_4 = \{\{\{1, 2, 3, 4\}\},\ \{\{1, 2, 3\}, \{1, 3, 4\}\},\ \{\{1, 2, 4\}, \{2, 3, 4\}\}\}$$

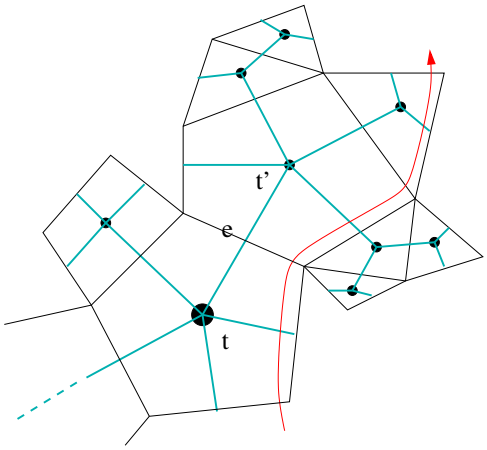

FIGURE 7. Dual tree example.

We present two proofs of Theorem 2.1: one by constructing an inverse — in Section 4 we show how to determine the flip equivalence class from the permutation; and one by direct geometrical arguments — see Section 6. We first establish machinery used by both.

3. Machinery for proof of Theorem 2.1

The *open dual* $\gamma(T)$ of tiling T is the dual graph of T regarded as a plane-embedded graph (see e.g. [7]) excluding the exterior face (so restricted to vertex set T). See Figure 7 for an example.

Lemma 3.1. *Graph $\gamma(T)$ is a tree.*

Proof. By construction the boundary of plane-embedded graph $\gamma(T)$ (see e.g. [21]) has the same number of components as the boundary of T. □

A *proper tiling* is a tiling with at least two tiles. An *ear* in a proper tiling T is a tile with one edge a diagonal. An r-ear is an r-gonal ear.

Corollary 3.2. *Every proper tiling has at least 2 ears.* □

3.1. **Elementary properties of strands.** Consider a tiling T. Note that a tile t in T and an edge e of t determine a strand of the $\boldsymbol{\sigma}(T)$ construction — the strand leaving t through e. Now, when a strand s leaves a tile t through an edge e it passes to an adjacent tile t' (as in Figure 7), or exits P and terminates. We associate a (possibly empty) branch $\gamma_{t,e}$ of $\gamma(T)$ to this strand at e: the subgraph accessible from the vertex of t' without touching t. Note that the continuation of the strand s leaves t' at some edge e' distinct from e, and that $\gamma_{t',e'}$ is a subgraph of $\gamma_{t,e}$.

Lemma 3.3. *Consider the strand construction on a tiling. After leaving a tile at an edge, a strand does not return to cross the same edge again.*

Proof. Consider the strand as in the paragraph above. If the strand exits the polygon P at e we are done. Otherwise, since the sequence of graphs γ_{t^i,e^i} associated to the passage of the strand is a decreasing sequence of graphs, containing each other, it eventually leaves P and terminates in some tile of a vertex of $\gamma_{t',e'}$ and so does not return to t. □

An immediate consequence of Lemma 3.3 is the following:

Corollary 3.4. *A strand of a tiling T can only use one strand segment of a given tile of T.*

Lemma 3.5. *Let $T \in A_n$ be a tiling of an n-gon. Then the strands of $\overrightarrow{\boldsymbol{\sigma}}(T)$ have the following properties* [25, §14]*: (i) Crossings are transversal and the strands crossing a given strand alternate in direction. (ii) If two strands cross twice, they form an oriented digon. (iii) No strand crosses itself.*

Proof. The first two properties follow from the construction. That no strand crosses itself follows from Corollary 3.4. Note that the underlying polygon can be drawn convex, in which case strands are left-turning. The requirement that there are no unoriented lenses follows from the fact that strands are left-turning in this sense. (Remark: our main construction is unaffected by non-convexity-preserving ambient isotopies, but the left-turning property is only preserved under convexity preserving maps.) □

We write $x \rightsquigarrow y$ for a strand starting at vertex x and ending at vertex y. Thus if $x \rightsquigarrow y$ is a strand of tiling T and σ is $\boldsymbol{\sigma}(T)$ then this strand determines $\sigma(x) = y$.

If a list of vertices is ordered minimally clockwise around the polygon, we will often just say clockwise, for example $(7, 1, 2)$ is ordered minimally clockwise. To emphasise that vertices x_1, x_2, x_3 are ordered minimally clockwise, we will repeat the "smallest" element at the end: $x_1 < x_2 < x_3 < x_1$.

Definition 3.6. Let q be a vertex of a polygon with strand diagram.
(1) We say that a strand $x \rightsquigarrow y$ *covers* q if we have $x < q < y < x$ minimally clockwise.
(2) We say that $x \rightsquigarrow y$ *covers* strand $x' \rightsquigarrow y'$ if $x < x' < y' < y < x$ or $x < y' < x' < y < x$.

3.2. **Factorisation Lemma.**

Consider the two strands s_1, s_2 passing through an edge e of a tile t. We say these strands are 'antiparallel at e'; and consider the 'parallel' strand s_1 and antistrand $\overline{s_2}$ both moving into t from e. Examples:

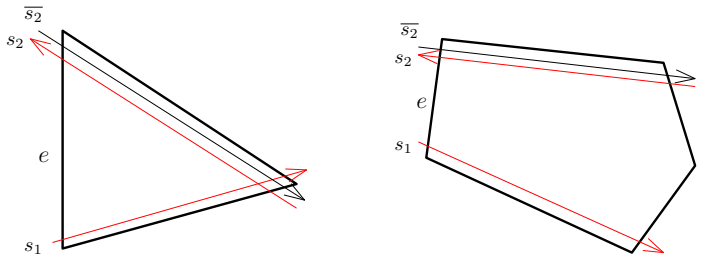

Lemma 3.7 ('Lensing Lemma'). *(I) Let strand segments s_1 and s_2 be antiparallel at an edge e of a tile t in a polygon tiling T. Traversing the two segments in the direction from e into the tile t, they do one of the following: (a) if t is a triangle the segments cross in t and do not meet again; (b) if t is a quadrilateral the segments leave t antiparallel in the opposite edge; (c) if $|t| > 4$ they leave t in different edges and the strands do not cross thereafter.*
(II) In any polygon tiling T, two strands cross at most twice. If two strands cross twice then (i) they pass through a common edge e; (ii) the crossings occur in triangles, on either side of e, with only quadrilaterals between.

Proof. (I) See the figure. Note that in cases (a) and (c) the strands pass out of t through different edges and hence into different subpolygons. Now use Lemma 3.3.
(II) Every crossing has to occur in a tile. If two strands enter a tile across different edges, they have not crossed before entering into the tile (Lemma 3.1). The claim then follows from (I). □

Lemma 3.8. *Let T be a tiling of an n-gon and $\sigma = \boldsymbol{\sigma}(T)$. Then (a) σ has no fixed points and (b) there is no i with $\sigma(i) = i + 1$.*

Proof. (a) Follows from the left-turning property (cf. Proof of Lemma 3.5). (b) Consider the tile with edge $e = [i, i + 1]$. The strand starting at i and the strand ending at $i+1$ have segments in the same tile and hence differ by Corollary 3.4. □

Lemma 3.9 ('Factorisation Lemma'). *Let P be a polygon and T_1, T_2 two tilings of P. Assume that there exists a diagonal $e = [i, j]$ in T_1 and T_2. Denote by P' the polygon on vertices $\{i, i + 1, \ldots, j - 1, j\}$. We have:*
$\boldsymbol{\sigma}(T_1) = \boldsymbol{\sigma}(T_2) \Longrightarrow \boldsymbol{\sigma}(T_1|_{P'}) = \boldsymbol{\sigma}(T_2|_{P'})$.

Proof. Consider Figure 8. The only way a strand of $\overrightarrow{\boldsymbol{\sigma}}(T_1)$ passes out of P' is through e, and there is exactly one such strand (and one passing in). This strand is non-returning by Lemma 3.3, so its endpoints are identifiable from $\sigma = \boldsymbol{\sigma}(T_1)$ as the unique vertex pair k, l with $\sigma k = l$ and with k in P' and l not. Apart from this and the corresponding 'incoming' pair with $\sigma k' = l'$, all other strand endpoint pairs of $\overrightarrow{\boldsymbol{\sigma}}(T_1|_{P'})$ are as in $\boldsymbol{\sigma}(T_1)$ and hence agree with $\overrightarrow{\boldsymbol{\sigma}}(T_2|_{P'})$ if $\boldsymbol{\sigma}(T_1) = \boldsymbol{\sigma}(T_2)$. Indeed, if $\boldsymbol{\sigma}(T_1) = \boldsymbol{\sigma}(T_2)$ then $\boldsymbol{\sigma}(T_2)$ identifies the same two pairs k, l and k', l'. At this point it is enough to show that the image of vertex k under $\overrightarrow{\boldsymbol{\sigma}}(T_1|_{P'})$, which is either vertex i or j, is determined by σ (since the determination will then be the same for $\overrightarrow{\boldsymbol{\sigma}}(T_2|_{P'})(k)$). If $k \geq l'$ then the strands $k \rightsquigarrow l$ and $k' \rightsquigarrow l'$ cross over

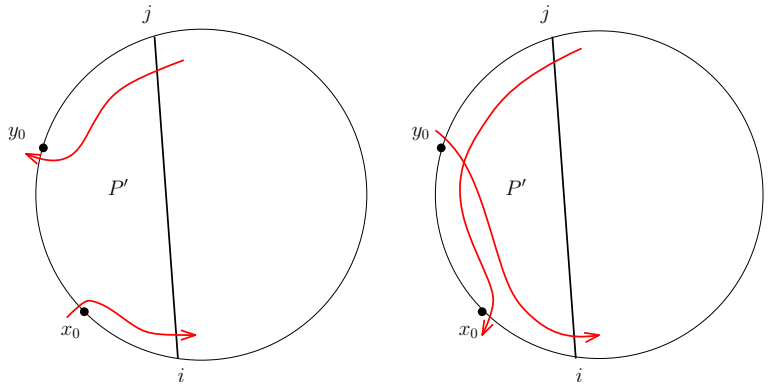

FIGURE 8. Schematic for two strands passing through diagonal $e = [i, j]$

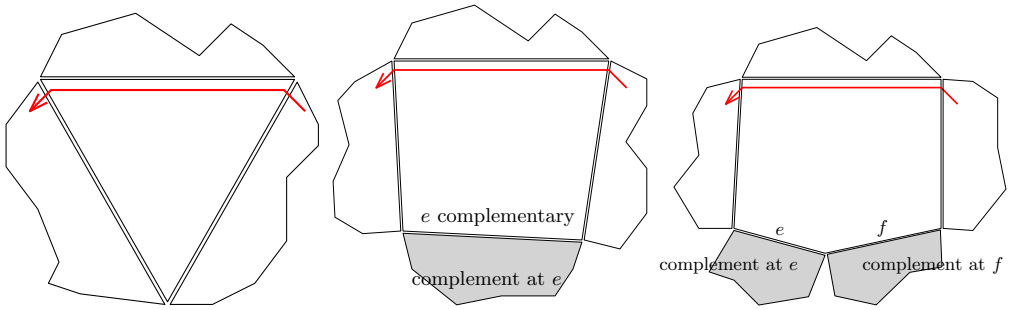

FIGURE 9. Tiles with complementary edges and their complements

each other in P', since otherwise they have the wrong orientation at e — see Fig.8. Thus the image of k is determined (it is i). If $k < l'$ then the image is determined similarly (this time non-crossing is forced and the image is j). □

3.3. **Properties of strands and tiles.**

We will say that a vertex in polygon P is *simple* in tiling T if it is not the endpoint of a diagonal. We will say that an edge $e = [i, i+1]$ of P is a *simple edge* in T if both vertices are simple.

Lemma 3.10. *A strand $i+1 \rightsquigarrow i$ arises in $\boldsymbol{\sigma}(T)$ if and only if the edge $[i, i+1]$ is simple.*

Proof. If $[i, i+1]$ is simple in T, the claim follows by construction. If i is not simple, then the strand ending at i contains the strand segment of the diagonal $[j, i]$ of T with $j < i-1$ maximal clockwise and has starting point in $\{j, j+1, \ldots, i-2\}$. Similarly, if $i+1$ is not simple, the strand starting at $i+1$ contains the strand segment of the diagonal $[i+1, k]$ with $k > i+2$ minimal anticlockwise. Its ending point is among $\{i+3, \ldots, k\}$. □

In general a strand passes through a sequence of tiles. At each such tile it is parallel to one edge and passes through the two adjacent edges. Any remaining edges in the tile are called *complementary* to the strand. Each of these complementary edges defines a sub-tiling — the tiling of the part of P on the other side of the edge. We call this the *complement to the corresponding edge*. Note that the strand covers every vertex in this sub-tiling. See for example Figure 9. We deduce:

Lemma 3.11. *(I) A strand $i \rightsquigarrow i+2$ passes only through triangles.*
(II) A strand $i \rightsquigarrow i+3$ passes through one quadrilateral (with empty complement) and otherwise triangles.
(III) A strand $i \rightsquigarrow i+4$ passes through one quadrilateral (with a complementary triangle) or two quadrilaterals or one pentagon (with empty complement), and otherwise triangles.
(IV) A strand $i \rightsquigarrow i+k$ passes through a tile sequence Q_i such that

$$k - 2 \geq \sum_i (|Q_i| - 3)$$

(the non-saturation of the bound corresponds to some tiles having non-empty complement). □

Example 3.12. As an illustration for Lemma 3.11 consider Figure 5. Both tilings have a strand $6 \rightsquigarrow 9$, illustrating the case $k = 3$.
In the tiling on the left, there is a strand $13 \rightsquigarrow 3$, it passes through one quadrilateral with complementary triangle $\{14, 1, 2\}$.

Lemma 3.13. *Let $T \in A_n$ and $\sigma = \boldsymbol{\sigma}(T)$. Then $\sigma(i) = i + 2$ if and only if there exists $T' \in [T]_\Delta$ with a 3-ear at vertex $i + 1$.*

Proof. If: T' has a strand direct from i to $i + 2$ in the given ear. Note that all other tilings in $[T']_\Delta$ have only triangles incident at $i + 1$ (since a neighbourhood of $i + 1$ lies in the triangulated part). One sees from the construction that these tilings all have a strand from i to $i + 2$. See (a):

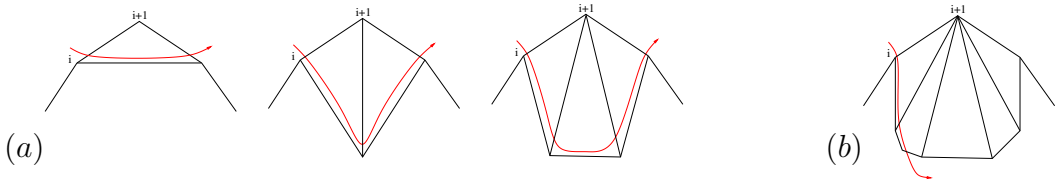

(a) (b)

Only if: If there is no such T' in $[T]_\Delta$ then among the tiles incident at $i+2$ is one with order $r > 3$. The strand from i passes into P at the first tile incident at $i+1$. If this is a triangle then the strand passes into the second tile, and so on. Thus eventually the strand meets a tile of higher order — see (b) above. But then by Lemma 3.11 we have $i \rightsquigarrow i + k$ with $k > 2$. □

For given n let us write τ for the basic cycle element in Σ_n: $\tau = (1, 2, ..., n)$. The following is implicit in [29], and is a corollary to Lemma 3.11.

Lemma 3.14. *Let T be an arbitrary triangulation of an n-gon. Then the permutation $\boldsymbol{\sigma}(T)$ associated to T is induced by $i \mapsto i + 2$, $1 \leq i \leq n$ (reducing mod n). Indeed, for $T \in A_n$, $\boldsymbol{\sigma}(T) = \tau^2$ if and only if T is a triangulation.*

Definition 3.15. A *run* is a subsequence of form $i-1, i-2, ..., i-r+1$ in a cycle of a permutation of S_n. A maximal subsequence of this form is an *r-run at i*.

In Figure 5, both permutations have a 3-run at 9.

Lemma 3.16. *Let $T \in A_n$, and $\sigma = \boldsymbol{\sigma}(T)$. We have*
i) σ contains a cycle of length $\geq r$, where $r \geq 2$, with an r-run at $j \iff [j-1, j-2]$, $[j-2, j-3], \ldots, [j-r+2, j-r+1]$ is a maximal sequence of simple edges in T;
ii) Assume $\boldsymbol{\sigma}(T)$ is as in (i) and $r < n-1$. Then TFAE
(a) $[j-r, j] \in T$; (b) $\{j-r, j-r+1, \ldots, j\}$ is an $(r+1)$-ear in T; (c) $\sigma(j-r) = j$.

Note that the case $r = 2$ occurs if $j-1$ is simple, while the edge $[j-1, j-2]$ is not simple - a triangular ear.

Proof. i) The implication $\Longleftarrow$ follows by construction. Implication $\Longrightarrow$ follows from Lemma 3.10.

ii) Observe that the the assumptions in ii) are consistent with (b).
(a) $\Longrightarrow$ (b) follows with i). (b) $\Longrightarrow$ (c) follows from the construction.
To show (c) $\Longrightarrow$ (a) first note that by the assumptions, j and $j+r$ are not simple. Among the diagonals incident with j consider the diagonal $[j, q_1]$ with endpoint q_1 maximal (and clockwise) from j. Among the diagonals incident with $j-r$ consider the diagonal $[q_2, j-r]$ with q_2 minimal (and anticlockwise) from $j-r$. If $q_1 = j-r$ (and hence $q_2 = j$), we are done. So assume for contradiction that $j < q_1 \leq g_2 < j-r < j$. Both diagonals are edges of a common tile Q containing the simple edges $[j-1, j-2]$, $[j-2, j-3], \ldots, [j-r+2, j-r+1]$. Consider the strand starting at $j-r$. It leaves the tile Q in $\{q_1+1, \ldots, q_2\}$. By Corollary 3.4 it cannot return back into Q, and so its endpoint is different from j. □

4. Inductive proof of Theorem

One proof strategy for the main theorem (Theorem 2.1) is as follows. We assume the theorem is true for orders $m < n$ (the induction base is clear).

The 'If' part follows from the Factorisation Lemma (Lemma 3.9) and Lemma 3.14.

For the 'Only if' part proceed as follows. Consider T_1, T_2 with $\sigma = \boldsymbol{\sigma}(T_1) = \boldsymbol{\sigma}(T_2)$. Note that T_1 has an ear, either triangular or bigger (Lemma 3.2). Pick such an ear E. Consider the cases (i) $|E| = 3$; (ii) $|E| \neq 3$.
(i) If E is triangular in T_1 then $\sigma = \boldsymbol{\sigma}(T_1)$ has $i \rightsquigarrow i+2$ at the corresponding position. Thus so does $\boldsymbol{\sigma}(T_2) = \boldsymbol{\sigma}(T_1)$, and hence there is a T_2' in $[T_2]_\Delta$ also with this ear, by Lemma 3.13. Note that $\boldsymbol{\sigma}(T_2') = \boldsymbol{\sigma}(T_2)$ since $T_1 \sim_\Delta T_2$.

Since $T_1 \setminus E$ and $T_2' \setminus E$ are well defined we have $\boldsymbol{\sigma}(T_1 \setminus E) = \boldsymbol{\sigma}(T_2' \setminus E)$ by the Factorisation Lemma (Lemma 3.9). That is, the Scott permutations $\boldsymbol{\sigma}(T_1)$ and $\boldsymbol{\sigma}(T_2')$ of T_1 and T_2' agree on the part excluding this triangle. But then $[(T_1 \setminus E)]_\Delta = [(T_2' \setminus E)]_\Delta$ (i.e. the restricted tilings agree up to triangulation) by the inductive assumption. Adding the triangle back in we have $[T_1]_\Delta = [T_2']_\Delta$. But $[T_2']_\Delta = [T_2]_\Delta$ and we are done for this case.
(ii) If ear E is not triangular in T_1 then T_2 has an ear in the same position by Lemma 3.16. The argument is a direct simplification of that in (i), considering $T_1 \setminus E$ and $T_2 \setminus E$. □

5. Geometric properties of tiles and strands

Definition 5.1. Fix n. Then an increasing subset $Q = \{q_1, q_2, ..., q_r\}$ of $\{1, 2, ..., n\}$ defines two partitions:

$$I(Q) = \{[q_1, \dots, q_2), [q_2, \dots, q_3), \dots, [q_r, \dots, q_1)\}$$
$$J(Q) = \{(q_1, \dots, q_2], (q_2, \dots, q_3], \dots, (q_r, \dots, q_1]\}$$

We denote the parts by $I_i(Q) := [q_i, \dots, q_{i+1})$ and $J_i(Q) := (q_i, \dots, q_{i+1}]$, for $i = 1, \dots, r$.

Such partitions arise from tilings: Let $Q \in A_n$. Then the vertices of Q partition the vertices of P in two ways. Consider the edge $e = [q_i, q_{i+1}]$ of Q. In the complement to e, there are $q_{i+1} - q_i$ strands starting at vertices in $I_i(Q)$ and the same number of strands ending at the vertices in $J_i(Q)$. Among them, $q_{i+1} - q_i - 1$ remain in the complement. For an example, see Figure 10.

Using this notation, we get an alternative proof for Corollary 3.4 stating that a strand of a tiling can only use one strand segment of a given tile: Let Q be a tile of a tiling $T \in A_n$ and let $q_1, \dots, q_r$ be its vertices, $r \geq 3$, $q_1 < q_2 < \cdots q_r < q_1$. Assume strand $x \rightsquigarrow y$ involves a strand segment of Q, say parallel to the edge $[q_{i-1}, q_i]$. By construction, this strand segment is oriented from q_i to q_{i-1}. We claim that the strand then necessarily starts in $I_i(Q)$ and ends in $J_{i-2}(Q)$. Consider the edge $[q_{i-2}, q_{i-1}]$ of Q: the only place for a strand to leave $J_{i-2}(Q)$ is near the vertex q_{i-2}. By the orientation of strand segments in tiles, strand $x \rightsquigarrow y$ could only leave near q_{i-2} if $q_{i-2} = q_{i-1}$ — a contradiction. Hence $y \in J_{i-2}(Q)$. A similar argument shows $x \in I_i(Q)$.

Remark 5.2. Let T be a tiling of P, with tile Q inducing partitions as above. There are two types of strands regarding these partitions. Let $x \rightsquigarrow y$ be a strand starting in $I_{i_1}(Q)$ and ending in $J_{i_2}(Q)$ for some i_1, i_2. Then we either have $i_1 = i_2$ or $i_1 = i_2 + 2$ (by the preceding argument or by Corollary 3.4). The case $i_1 = i_2 + 2$ is illustrated in Figure 10 for Q a pentagon.

Definition 5.3. Let Q be a tile of a tiling T of an n-gon. If a strand $x \rightsquigarrow y$ of T uses a strand segment of Q, we say that the strand $x \rightsquigarrow y$ is a *long strand for* Q.

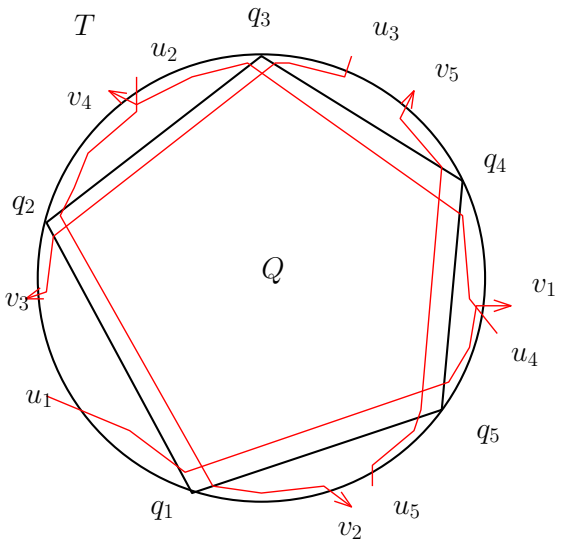

FIGURE 10. Tile inducing partition and long strands for Q

If for the partitions induced by Q, $x \in I_i$, then $y \in J_{i-2}$ if $x \rightsquigarrow y$ is a long strand for Q and $y \in J_i(Q)$ otherwise, cf. Remark 5.2.

Lemma 5.4. *Let Q be an r-tile of a tiling of P with vertices $q_1 < \cdots < q_r < q_1$ clockwise. Then every long strand $x \rightsquigarrow y$ with respect to Q covers exactly $r-2$ vertices of Q and there are exactly two vertices q_{i-1}, q_i for every such strand with $y \leq q_{i-1} < q_i \leq x < y$ (clockwise).*

Proof. If s is a long strand for Q with $x \rightsquigarrow y$, then there exists i such that $x \in I_i(Q) = [q_i, \ldots, q_{i+1})$ and $y \in J_{i-2}(Q) = (q_{i-2}, \ldots, q_{i-1}]$ (reducing the index mod n), hence it covers $q_{i+1}, q_{i+2}, \ldots, q_{i-2}$. For an illustration, see Figure 10. □

6. Geometric Proof of Theorem

We now use geometric properties of tilings to prove the "only if" part of Theorem 2.1. The maximum tile size of tiling T is denoted $r(T)$. For two tilings T_1, T_2 and $r_i = r(T_i)$, the case $r_1 \neq r_2$ is covered in Lemma 6.2; and $r := r_1 = r_2$ follows from Corollary 6.3 and Lemma 6.4. We first prove an auxiliary result.

Lemma 6.1. *(a) Consider a tiling T in A_n with a diagonal $e = [s_1, s_2]$. For each vertex q with $s_1 < q < s_2 < s_1$, we get a strand $s : y \rightsquigarrow z$ in $\boldsymbol{\sigma}(T)$ covering q, with $s_1 \leq y < q < z \leq s_2 < s_1$.*
(b) Consider T, q, s as in (a) and a further tiling T' of P containing a tile Q such that $\dim(Q \cap e) = 1$ and $q \in Q$. If $\boldsymbol{\sigma}(T')$ contains a strand with $y \rightsquigarrow z$ as in (a), it is a long strand for Q (as defined in Definition 5.3).

Proof. (a) Let $e' = [n_1, n_2]$ be the shortest diagonal in T lying above q. Note, $s_1 \leq n_1 < q < n_2 \leq s_2 < s_1$. Consider the strand segment in $\boldsymbol{\sigma}(T)$ following e'

from n_1 to n_2 (see figure below). This induces a strand s with $y \rightsquigarrow z$, say. We claim $n_1 \leq y < q$ and $q < z \leq n_2$. To see this let $[x, n_1]$ be in T with $n_1 \leq x$ and $x \leq q$ maximal ($x = n_1 + 1$ possibly). Then s has its starting point among $\{n_1, n_1+1, \ldots, x-1\}$, because e' is the shortest diagonal above q. Let $[y, n_2]$ be in T with $y \leq n_2$ and $y \geq q$ minimal. Then s has its endpoint among $\{y+1, \ldots, n_2\}$, similarly.

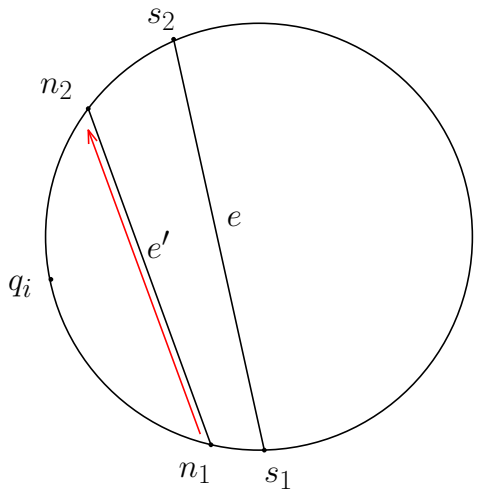

(b) Given (a), this follows immediately from Definition 5.3. □

Lemma 6.2. *Let T_1 and T_2 be two tilings of a polygon P with $\boldsymbol{\sigma}(T_1) = \boldsymbol{\sigma}(T_2)$. Then $r_1 = r_2$.*

Proof. Let $r = r_2$. In case $r_1 = 3$, the claim follows from Lemma 3.14: in this case, $\boldsymbol{\sigma}(T_1)$ is induced by $i \mapsto i+2$ and T_2 has to be a triangulation, too. Assume that $\boldsymbol{\sigma}(T_1) = \boldsymbol{\sigma}(T_2)$ and for contradiction, assume that $r_1 < r$. (Remark: By the above, we can assume $r > 4$.) We consider a tile Q of size r in T_2, with vertices $q_1, \ldots, q_r$. In T_1, we choose a tile S with $\dim Q \cap S > 1$. We write $\{s_1, ..., s_s\}$ for the vertices of S, with $|S| = s < r$.

By this construction there is an edge $e = [s_1, s_2]$ of S and $q_i \in Q$ with $s_1 < q_i < s_2 < s_1$. There is, therefore, a strand with $y \rightsquigarrow z$ in $\boldsymbol{\sigma}(T_1)$ covering q_i, as in Lemma 6.1.

Since $\boldsymbol{\sigma}(T_1) = \boldsymbol{\sigma}(T_2)$, under the tiling T_2 there exists a strand with $y \rightsquigarrow z$ covering q_i. By Lemma 6.1(b) it is a long strand for Q. Consider the subpolygon P' on the vertices $y, y+1, \ldots, z$, i.e. with interior edge $e' = [y, z]$. We have shown in Lemma 5.4 that $r-2$ vertices of Q lie in P', w.l.o.g. these are $\{q_1, \ldots, q_{r-2}\}$. Furthermore these $r-2$ vertices are different from y, z (again Lemma 5.4). Thus, P' has at least r vertices.

We consider the diagonals in T_1 with endpoints among $y, y+1, \ldots, z$, covering at least one of $\{q_1, \ldots, q_{r-2}\}$. Not all of these diagonals cover all $r-2$ vertices (otherwise we would get a tile of size r in T_1, specifically $\{a, q_1, \ldots, q_{r-2}, b\}$ where $[a, b]$ is the shortest covering diagonal). So let $e'' = [n_1, n_2]$ with $y \leq n_1 < n_2 \leq$

$z < y$ cover q_{l_1}, say, but not q_{l_2}. By the same argument as above, this implies that there exists a strand with $y_2 \rightsquigarrow z_2$ in $\boldsymbol{\sigma}(T_1)$, with $n_1 \leq y_2 < q_{l_1} < z_2 \leq n_2 < n_1$. We are in the situation here:

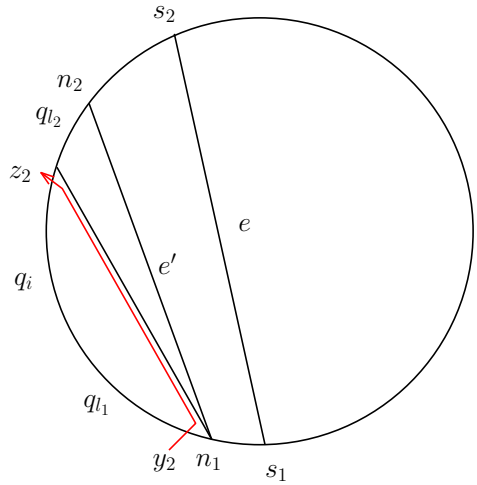

In $\boldsymbol{\sigma}(T_2)$, the assumed strand from y_2 to z_2 is a long strand for Q again by Lemma 6.1. As before, this implies that among the vertices $n_1+1, n_1+2, \ldots, n_2-1$, there are $r-2$ vertices of Q. But we already have q_{r-1}, q_r and q_{l_2} lying outside. A contradiction. □

Corollary 6.3. *Let $\boldsymbol{\sigma}(T_1) = \boldsymbol{\sigma}(T_2)$. If in T_1 there exists an edge $e = [s_1, s_2]$ and in Q a tile of size ≥ 4 with $\dim Q \cap e = 1$, then either e is an edge of Q or e separates vertices of Q ($s_1 > q_x > s_2 > q_y > s_1$ for some x, y) and $|Q| = 4$.*

Proof. If e is not an edge of Q, we find vertices q_i and q_j of Q with $s_1 < q_i < s_2 < q_j < s_1$. We can thus use Lemma 6.1 and Lemma 5.4 for q_i and again for q_j to see that Q has $r-2$ vertices on the left side of e and $r-2$ vertices to the right of e, and that they all differ from s_1 and from s_2. □

Lemma 6.4. *Let T_1 and T_2 be two tilings of a polygon P with $\boldsymbol{\sigma}(T_1) = \boldsymbol{\sigma}(T_2)$ and assume $r_1 = r_2 = 4$. Then $[T_1]_\Delta = [T_2]_\Delta$.*

Proof. By Lemma 3.10 the positions of 4-ears in T_1 and T_2 agree, when $r_1 = r_2 = 4$. By the Factorisation Lemma (Lemma 3.9) we can remove (common) ears of size 4, to leave reduced tilings T_1' and T_2' of some P'. These necessarily have ears, but by Lemma 3.11, (up to equivalence) 3-ears can be chosen to be in the same positions in each tiling. Now iterate. □

Proof of Theorem 2.1. If the maximum tile sizes of T_1 and of T_2 differ, the claim follows from Lemma 6.2. So let $r = r_1 = r_2$ be the maximum tile size of T_1 and of T_2. If $r = 4$, Lemma 6.4 proves the claim. So assume that there are tiles of size $r > 4$ and consider such a tile Q in T_2. By Corollary 6.3 there are no diagonals of T_1 'intersecting' Q, so in T_1 we have a tile containing Q. Applying the same

argument with the tilings reversed we see that T_1 and T_2 agree on parts tiled with tiles of size > 4.

By the Factorisation Lemma (Lemma 3.9), we can remove all (common) ears of size > 4. Among the remaining (common) tiles of size at least 5, we choose a tile Q and a non-boundary edge e of Q, such that to one side of e, all tiles in T_1 and in T_2 have size at most four. Let P' be the union of these tiles of size ≤ 4. By the Factorisation Lemma we have $\boldsymbol{\sigma}(T_1 \mid_{P'}) = \boldsymbol{\sigma}(T_2 \mid_{P'})$ and by Lemma 6.4, $[T_1 \mid_{P'}] = [T_2 \mid_{P'}]$. We can remove P' and repeat the above until Q is a (common) ear - which can be removed, too. Iterating this proves the claim. □

7. On the image of the Scott map treated combinatorially

To give an intrinsic characterization of the image in Σ_n of the Scott map $\boldsymbol{\sigma} : A_n \to \Sigma_n$ for all n remains an interesting open problem. Note in particular that so far the map does not equip the image with a group structure (or indeed any algebraic structure). Here we report on one invariant which Theorem 2.1 gives us access to, namely the size of the image, which is given by $|Æ_n|$.

As an initial illustration we observe that:

Proposition 7.1. *The number of permutations arising from tiling an n-gon using one r-gon ($r > 3$) and triangles otherwise is $\binom{n}{r}$.*

Proof. By the main Theorem this is the same as enumerating the classes in $Æ_n$ of this type. Since the details of the triangulated part are irrelevant, the class is determined by choosing the vertices of the r-gon. Hence choosing r from n. □

Example 7.2. In total, there are 26 permutations arising from the 45 tilings of the hexagon: one from the empty tiling; 6 from tilings with one pentagon and one triangle; 15 from tilings with one quadrilateral and two triangles; 3 from tilings using two quadrilaterals; and 1 from the triangulation case.
Figure 2 contains examples of these tilings and the associated permutations.

In order to go further we will need some notation.

7.1. **Notation and known results.** Recall that an integer partition $\lambda = (\lambda_1, \lambda_2, \dots)$ has also the exponent notation:

$$\lambda = r^{\alpha_r}(r-1)^{\alpha_{r-1}} \cdots 2^{\alpha_2} 1^{\alpha_1}$$

A λ-*tiling* is a tiling with, for each d, α_d tiles that are $(d+2)$-gonal.

Recall that A_n is the complex of tilings of the n-gon. Define $a_n = |A_n|$. Write $A_n(m)$ (with $m \in \{0, 1, 2, \dots, n-3\}$) for the set (and $a_n(m)$ the number) of tilings with m diagonals. Write $A_n(\lambda)$ (with λ an integer partition of $n-2$) for the set of λ-tilings (thus with a m-gonal face for each row $\lambda_i = m-2$). Thus

$$A_n(m) = \bigcup_{\lambda \vdash n-2 \,:\, \lambda'_1 = m+1} A_n(\lambda) \tag{2}$$

Similarly recall $Æ_n$ is the set of classes of tilings under triangulated-part/flip equivalence. Write $Æ_n(m)$ for the set $A_n(m)$ under triangulated-part equivalence and $Æ_n(\lambda)$ the set $A_n(\lambda)$ under triangulated-part equivalence.

(7.3) The sequence a_n is the little Schröder numbers (see e.g. [30] and OEIS A001003). It is related to the Fuss–Euler combinatoric as follows. By [27] the number of tilings of the n-gon with m diagonals is

$$a_n(m) = \frac{1}{m+1}\binom{n+m-1}{m}\binom{n-3}{m} \tag{3}$$

($a_n(m) = q_m(1,n)$ from [27]). Thus in addition to the usual generating function

$$\sum_{n\geq 0} a_n x^n = \frac{1+x-\sqrt{1-6x+x^2}}{4x}$$

we have

$$a_n = \sum_{m=0}^{n} \frac{1}{m+1}\binom{n+m-1}{m}\binom{n-3}{m} \tag{4}$$

7.2. **Explicit construction of A_n.** Of greater use than an expression for the size of A_n is an explicit construction of all tilings. For this we shall consider a tiling in A_n to be as in the formal definition, i.e. to be the same as its set of arcs. This is the set of diagonals in the present polygon case, where we can represent an arc between vertices i, j unambiguously by $[i, j]$. In particular then we have an inclusion $A_{n-1} \hookrightarrow A_n$. The copy of A_{n-1} in A_n is precisely the subset of tilings in which vertex n is simple and there is no diagonal $[1, n-1]$.

There is a disjoint image $J(A_{n-1})$ of A_{n-1} in A_n given by $J(T) = T \cup \{[1, n-1]\}$. The set $A_{n-1} \sqcup J(A_{n-1})$ is the subset of A_n of elements in which n is simple. Consider in the complement the subset of tilings containing $[n-2, n]$. In this the vertex $n-1$ is necessarily simple. Thus this subset is the analogue $J_{n-1}(A_{n-1})$ of $J(A_{n-1})$ constructed with $n-1$ instead of n as the distinguished simple vertex. The practical difference is that (i) the image tilings have all occurences of $n-1$ replaced by n; (ii) the 'added' diagonal is $[n-2, n]$.

There remain in A_n the tilings in which n is not simple but there is not a diagonal $[n-2, n]$. Consider those for which there is a diagonal $[n-3, n]$. In the presence of this diagonal any tiling 'factorises' into the parts in the two subpolygons on either side of this diagonal. One of these has vertices $1, 2, ..., n-3$ and n, and so its tilings are an image of A_{n-2} where vertex $n-2$ becomes vertex n. The other has vertices $n-3, n-2, n-1, n$ and so has tilings from a shifted image of A_4, but has n simple (since $[n-3, n]$ is the first diagonal in the original tiling). Since n is simple, it is the part of that image coming from $A_3 \sqcup J(A_3)$. We write $2.K(A_3)$ for these two shifted copied of A_3. We write $2.K(A_3) \cdot A_{n-2}$ for the meld with tilings from A_{n-2} to construct the set of tilings of the original polygon.

n	Σ	$m=0$	1	2	3	4	5	6	7
3	1	1							
4	3	1	2						
5	11	1	5	5					
6	45	1	9	21	14				
7	197	1	14	56	84	42			
8	903	1	20	120	300	330	132		
9	4279	1	27	225	825	1485	1287	429	
10	20793	1	35	385	1925	5005	7007	5005	1430
n		1	$\frac{n(n-3)}{2}$	$\frac{\binom{n+1}{2}\binom{n-3}{2}}{3}$					

TABLE 1. Values of $a_n(m)$, and hence a_n, in low rank.

There now remain in A_n the tilings in which n is not simple but there is not a diagonal $[n-2,n]$ or $[n-3,n]$. Consider those for which there is a diagonal $[n-4,n]$. In the presence of this diagonal any tiling 'factorises' into the parts in the two subpolygons on either side of this diagonal. We have the obvious generalisation of the preceeding construction in this case, written $2.K(A_4)\cdot A_{n-3}$.

We may iterate this construction until all cases of diagonals from n are included. We have established the following.

Proposition 7.4. *Consider the list defined recursively by* $\mathbf{A}_3 = (\varnothing)$ *and*

$$\mathbf{A}_n \;=\; \mathbf{A}_{n-1} \cup J(\mathbf{A}_{n-1}) \cup J_{n-1}(\mathbf{A}_{n-1}) \cup \bigcup_{r=2}^{n-3} 2.K(\mathbf{A}_{r+1})\cdot \mathbf{A}_{n-r}$$

where set operations on lists are considered as concatenation in the natural order; $2.-$ *denotes the doubling as above;* $K()$ *denotes the relabeling of all vertices so that the argument describes a suitable subpolygon; and* $A\cdot B$ *denotes the meld of tilings from subpolygons as above. Then this list is precisely a total order of* A_n*.*

Proof. Noting the argument preceding the Proposition, it remains to lift the construction from the set to the list. But this requires only the interpretation of union as concatenation. □

7.3. **Tables for $A_n(\lambda)$.** The class sets $Æ_n$ are harder to enumerate than A_n. Practically, one approach is to list elements of A_n and organise by arrangement of their triangulated parts, which determines the class size. We first recall the numbers $a_n(m)$ of tilings of an n-gon with m diagonals: see Table 1. The main diagonal enumerates the top dimensional simplices in A_n. It counts triangulations and hence is the Catalan sequence C_n. The entries in the next diagonal correspond to tilings with a single quadrilateral and triangles else.

We will give the number of elements of $Æ_n(m)$ for small n in Table 2. In order to verify this it will be convenient to refine tables 1 and 2 by considering these

n	Σ	$m=0$	1	2	3	4	5	6	7
3	1	1							
4	2	1	1						
5	7	1	5	1					
6	26	1	9	15	1				
7	100	1	14	49	35	1			
8	404	1	20	112	200	70	1		
9	1691	1	27	216	654	666	126	1	
10	7254	1	35	375	1660	3070	1902	210	1

TABLE 2. Table of $Æ_n$ sizes up to $n = 10$.

numbers for fixed partitions λ. Specifically we subdivide each case of m from the previous tables according to λ, with the m-th composite entry written as a list of entries in the form $\frac{(\lambda_1,\lambda_2,\ldots)}{a_n(\lambda)}$ ranging over all λ with $|\lambda| = m$. Thus for example $\frac{(32)}{7}$ tells that $a_7((3,2)) = 7$. We include Table 3 for $A_n(\lambda)$ and Table 4 for $Æ_n(\lambda)$. Neither table is known previously. The a_n case is computed partly by brute force (and see below); verified in GAP [12], and checked using identity (2)).

For the purpose of computing $Æ_n$ a better filtration is by the partition describing the size of the connected triangulated regions. But this is even harder to compute in general.

7.4. **Formulae for $|Æ_n(\lambda)|$ for all n.**

In the λ notation Proposition 7.1 becomes

$$|Æ_n((r-2)1^{n-r})| \;=\; \binom{n}{r} \tag{5}$$

To determine the size of image of the Scott map for a polygon of a given rank, one strategy is to compute $Æ_n(\lambda)$ through $A_n(\lambda)$. While $A_n(\lambda)$ is also not known in general, we have a GAP code [12, 3] to compute any given case.

If in a tiling, there is at most one triangle, we have $Æ_n(\lambda) \cong A_n(\lambda)$. In the case of two triangles, the following result determines $|Æ_n(\lambda)|$ from tilings of the same type and from tilings where the two triangles are replaced by a quadrilateral:

Proposition 7.5. *Let* $\lambda = r^{\alpha_r}(r-1)^{\alpha_{r-1}}\cdots 2^{\alpha_2}1^{\alpha_1}$.
(i) If $\alpha_1 < 2$ *then* $|Æ_n(\lambda)| = a_n(\lambda)$.
(ii) If $\alpha_1 = 2$ *then*

$$|Æ_n(\lambda)| \;=\; a_n(\lambda) - (\alpha_2+1)a_n(\lambda 21^{-2})$$

(iii) If $\alpha_1 = 3$ *then*

$$|Æ_n(\lambda)| \;= a_n(\lambda) - (\alpha_2+1)a_n(\lambda 21^{-2}) + (\alpha_3+1)a_n(\lambda 31^{-3})$$

n	Σ	$\lvert\lambda\rvert=0$	1				2				3						4						5			6	7
3	1	(1)																									
		1	1																								
4	3	(2)	(1^2)																								
		1	2																								
5	11	(3)	(21)				(1^3)																				
		1	5				5																				
6	45	(4)	(31)	(2^2)			(21^2)				(1^4)																
		1	6	3			21				14																
7	197	(5)	(41)	(32)			(31^2)	(2^21)			(21^3)						(1^5)										
		1	7	7			28	28			84						42										
8	903	(6)	(51)	(42)	(3^2)		(41^2)	(321)	(2^3)		(31^3)	(2^21^2)					(21^4)						(1^6)				
		1	8	8	4		36	72	12		120	180					330						132				
9	4279	(7)	(61)	(52)	(43)		(51^2)	(421)	(3^21)	(32^2)	(41^3)	(321^2)	(2^31)				(31^4)	(2^21^3)					(21^5)			(1^7)	
		1	9	9	9		45	90	45	45	165	495	165				495	990					1287			429	
10	20793	(8)	(71)	(62)	(53)	(4^2)	(61^2)	(521)	(431)	(42^2)	(3^32)	(51^3)	(421^2)	(3^21^2)	(32^21)	(2^4)	(41^4)	(321^3)	(2^31^2)				(31^5)	(2^21^4)		(21^6)	(1^8)
		1	10	10	10	5	55	110	110	55	55	220	660	330	660	55	715	2860	1430				2002	5005		5005	1430

Table 3: Table of $A_n(\lambda)$.

TABLE 3. Table for size of $A_n(\lambda)$.

n	Σ	$\lvert\lambda\rvert=0$	1			2				3					4					5					6		7
3	1	(1)																								
		1																								
4	2	(2)	(1^2)																							
		1	1																							
5	7	(3)	(21)			(1^3)																				
		1	5			1																				
6	26	(4)	(31)	(2^2)		(21^2)				(1^4)																
		1	6	3		15				1																
7	100	(5)	(41)	(32)		(31^2)	(2^21)			(21^3)					(1^5)											
		1	7	7		21	28			35					1											
8	404	(6)	(51)	(42)	(3^2)	(41^2)	(321)	(2^3)		(31^3)	(2^21^2)				(21^4)					(1^6)						
		1	8	8	4	28	72	12		56	144				70					1						
9	1691	(7)	(61)	(52)	(43)	(51^2)	(421)	(3^21)	(32^2)	(41^3)	(321^2)	(2^31)			(31^4)	(2^21^3)				(21^5)					(1^7)	
		1	9	9	9	36	90	45	45	84	405	165			126	540				126					1	
10	7254	(8)	(71)	(62)	(53)	(4^2)	(61^2)	(521)	(431)	(42^2)	(3^22)	(51^3)	(421^2)	(3^21^2)	(32^21)	(2^4)	(41^4)	(321^3)	(2^31^2)		(31^5)	(2^21^4)		(21^6)		(1^8)
		1	10	10	10	5	45	110	110	55	55	120	550	275	660	55	210	1650	1210	252	1650	210	1			

Table 4: Table of $Æ_n(\lambda)$.

TABLE 4. Table for size of $Æ_n(\lambda)$

(iv) If $\alpha_1 = 4$ then

$$|Æ_n(\lambda)| = a_n(\lambda) - (\alpha_4+1)a_n(\lambda 41^{-4}) + (\alpha_3+1)a_n(\lambda 31^{-3}) + \binom{\alpha_2+2}{2} a_n(\lambda 221^{-4}) - (\alpha_2+1)a_n(\lambda 21^{-2})$$

Proof. (ii) Consider partitioning $A = A_n(\lambda)$ into a subset A' of tilings where the triangles are adjacent, and A'' where they are not. Evidently $|Æ_n(\lambda)| = |A'|/2 + |A''| = |A| - |A'|/2$. On the other hand in A' the triangles form a distinguished quadrilateral. For each element of $A_n(\lambda 21^{-2})$ we get $\alpha_2 + 1$ ways of selecting a distinguished quadrilateral. There are two ways of subdividing this quadrilateral, thus $|A'| = 2(\alpha_2+1)a_n(\lambda 21^{-2})$. □

Example 7.6. Proposition 7.5 determines $|Æ_8(2^21^2)|$. Here $A_8(2^21^2)$ gives an overcount because of the elements where the two triangles are adjacent. Only one representative of each pair under flip should be kept. These are counted by marking one quadrilateral in each element of $A_8(2^3)$. There are three ways of doing this, so we have

$$|Æ_8(2^21^2)| = |A_8(2^21^2)| - 3|A_8(2^3)| = 180 - 36$$

from Table 3. Similarly $|Æ_8(41^2)| = |A_8(41^2)| - |A_8(42)| = 36 - 8$.

(7.7) *Proof of (iii):* For $\alpha_1 = 3$ partition $A = A_n(\lambda)$ into subset A' of tilings with three triangles together; A'' with two together; and A''' with all separate. We have $|Æ_n(\lambda)| = |A'''| + |A''|/2 + |A'|/5$. That is,

$$|Æ_n(\lambda)| = |A| - |A''|/2 - 4|A'|/5. \tag{6}$$

Considering the triangulated pentagon in a tiling T in A' as a distinguished pentagon we have

$$|A'| = 5(\alpha_3+1)a_n(\lambda 31^{-3}). \tag{7}$$

Next aiming to enumerate A'', consider $\lambda 21^{-2}$, somewhat as in the proof of (ii), but here there is another triangle, which must not touch the marked 4-gon. Let us write $(\alpha_2+1)A(\lambda 21^{-2})$ to denote a version of $A(\lambda 21^{-2})$ where one of the quads is marked. There are two ways of triangulating the marked quad, giving $X = 2(\alpha_2+1)A(\lambda 21^{-2})$, say. Consider the subset B of X of tilings where the marked quadrilateral and triangle are not adjacent.

Claim: $B \cong A''$.

Proof: The construction (forgetting the mark) defines a map $B \to A''$. Marking the adjacent pair of triangles in an element of A'' gives a map $A'' \to B$ that is inverse to it. □

The complementary subset C of X has quadrilateral and triangle adjacent. Elements map into A' by forgetting the mark.

Claim: C double counts A', i.e. the forget-map is surjective but not injective.

Proof: There are 5 ways the quadrilateral and triangle can occupy a pentagon

together, and two ways of triangulating the quad. The cases can be written out, and this double-counts the triangulations of the pentagon. □

Altogether $A'' = B = X - C = X - 2A'$ so

$$\text{Æ}(\lambda) = A(\lambda) - ((1/2)X - A') - (4/5)A' = A(\lambda) - (X/2) + A'/5$$
$$= A(\lambda) - (\alpha_2 + 1)A(\lambda 21^{-2}) + (\alpha_3 + 1)A(\lambda 31^{-3})$$

□

(7.8) *Proof of (iv):* For $\alpha_1 = 4$ partition $A = A(\lambda)$ by $A = A^4 + A^{31} + A^{22} + A^{211} + A^{1111}$ so that

$$\text{Æ} = A^4/C_4 + A^{31}/C_3 + A^{22}/C_2^2 + A^{211}/C_2 + A^{1111} = A - \frac{13}{14}A^4 - \frac{4}{5}A^{31} - \frac{3}{4}A^{22} - \frac{1}{2}A^{211}$$

By direct analogy with (7) we claim

$$A^4 = 14(\alpha_4 + 1)A(\lambda 41^{-4})$$

Next consider $X = 5(\alpha_3 + 1)A(\lambda 31^{-3})$, marking one 5-gon, and then triangulating it. We have a subset B where the 5-gon and triangle are not adjacent; and complement C.

Claim: $B \cong A^{31}$. This follows as in the proof of part (iii).

The complement C maps to A^4 by forgetting the mark.

Claim: $14|C| = 30|A^4|$.

Proof: There are 6 ways the 5-gon and triangle can occupy a hexagon together, and 5 ways to triangulate the 5-gon. This gives 30 marked cases, which pass to 14 triangulations.

So far we have that

$$A^{31} = B = X - C = 5(\alpha_3 + 1)A(\lambda 31^{-3}) - \frac{30}{14}A^4$$

It remains to determine A^{22} and A^{211}.

(7.9) Next consider $Y = 4\binom{(\alpha_2+2)}{2}A(\lambda 221^{-4})$, marking two 4-gons, and then triangulating them. Subset D has the 4-gons non-adjacent; and E is the complement.

Claim: $D \cong A^{22}$. This follows similarly as the statement on B.

The complement E maps to A^4 by forgetting the marks.

Claim: $14|E| = 12|A^4|$.

Proof: There are 3 ways the 4-gons can occupy a hexagon together, and 4 ways to triangulate them. (NB the map is not surjective — not every triangulation of a hexagon resolves as two quadrilateral triangulations — but we only need to get the count right. We always get 12 out of 14 possible in each case.)

So far we have

$$A^{22} = Y - E = 4\binom{\alpha_2 + 2}{2}A(\lambda 221^{-4}) - \frac{12}{14}|A^4|$$

Next we need A^{211}.

(7.10) Next consider $Z = 2(\alpha_2+1)A(\lambda 21^{-2})$, marking a 4-gon and triangulating it. Subset F has the three parts non-adjacent. Subset G has the 4-gon and one triangle adjacent. Subset G' has the two triangles adjacent. Subset H has all three parts adjacent:

$$Z = F + G + G' + H$$

Claim: $F \cong A^{211}$. This follows similarly as the statements on B and on C.

The set G maps to A^{31}, and G' to A^{22}, and H to A^4, by forgetting the marks.

Claim: (a) $|G| = 2|A^{31}|$ and (b) $|G'| = 2|A^{22}|$ and (c) $14|H| = 42|A^4|$.

Proof: (a) Elements of G pass to tilings with triangulations of a 5-gon and a separate triangle. The collection of them triangulating a given 5-gon and triangle has order 10 (5 ways to mark a quadrilateral in the 5-gon, then two ways to triangulate it). On the other hand the number of triangulations of the same region in A^{31} is 5.

(b) Elements of G' pass to tilings with triangulations of two 4-gons. The collection of such gives all these triangulations. Each one occurs twice in G' since the triangulation of the two 4-gon regions can arise in G' with one or the other starting out as the marked 4-gon.

(c) Elements of H pass to tilings with triangulations of a hexagon. The collection of such gives $A_6(21^2) = 21$ ways of tiling the hexagon with quadrilateral and two triangles, then two ways of tiling the quad. On the other hand there are 14 triangulations of this hexagon in A^4.

We have $A^{211} = Z - (G+G'+H) = 2(\alpha_2+1)A(\lambda 21^{-2}) - (\frac{2}{1}A^{31} + \frac{2}{1}A^{22} + \frac{42}{14}A^4)$.

Altogether now

$$\text{Æ}(\lambda) = A - \frac{13}{14}A^4 - \frac{4}{5}A^{31} - \frac{3}{4}A^{22} - \frac{1}{2}A^{211}$$

$$= A(\lambda) - \frac{13}{14}A^4 - \frac{4}{5}\left(5(\alpha_3+1)A(\lambda 31^{-3}) - \frac{30}{14}A^4\right) - \frac{3}{4}\left(4\binom{\alpha_2+2}{2}A(\lambda 221^{-4}) - \frac{12}{14}|A^4|\right)$$
$$- \frac{1}{2}\left(2(\alpha_2+1)A(\lambda 21^{-2}) - (\frac{2}{1}A^{31} + \frac{2}{1}A^{22} + \frac{42}{14}A^4)\right)$$

$$= A(\lambda) + \frac{-13+21}{14}A^4 + \frac{1}{5}\left(5(\alpha_3+1)A(\lambda 31^{-3}) - \frac{30}{14}A^4\right) + \frac{1}{4}\left(4\binom{\alpha_2+2}{2}A(\lambda 221^{-4}) - \frac{12}{14}|A^4|\right)$$
$$- \frac{1}{2}\left(2(\alpha_2+1)A(\lambda 21^{-2})\right)$$

$$= A(\lambda) + \frac{-13-6-3+21}{14}A^4 + (\alpha_3+1)A(\lambda 31^{-3}) + \binom{\alpha_2+2}{2}A(\lambda 221^{-4}) - (\alpha_2+1)A(\lambda 21^{-2})$$

$$= A(\lambda) - (\alpha_4+1)A(\lambda 41^{-4}) + (\alpha_3+1)A(\lambda 31^{-3}) + \binom{\alpha_2+2}{2}A(\lambda 221^{-4}) - (\alpha_2+1)A(\lambda 21^{-2})$$

□

7.5. **Tables for Æ_n.**

Proposition 7.11. *The numbers Æ_n for $n < 11$ are given in Table 2.*

Proof. The numbers $a_n(\lambda)$ are given in Table 3 by a GAP calculation [3]. The numbers in Table 4 then follow from formula (5) and Proposition 7.5. Table 2 follows immediately. □

7.6. **On asymptotics.** We determined in tables 2, 4 the sizes of the image of the Scott map in low rank. Of course the ratio of successive sizes of the formal codomains grows with n as $|\Sigma_n|/|\Sigma_{n-1}| = n$. In the next table we consider the ratios of two consecutive entries of the sequence $|\text{Æ}_n|_n$.

n	3	4	5	6	7	8	9	10
$\lvert\text{Æ}_n\rvert$	1	2	7	26	100	404	1691	7254
$\lvert\text{Æ}_n\rvert/\lvert\text{Æ}_{n-1}\rvert$		2	3.5	3.71	3.85	4.04	4.19	4.29

(7.12) A paradigm for this is the Catalan combinatoric C_n (see e.g. [30]), which can also be equipped with an inclusion in the permutations Σ_n — see e.g. [19, 28] (NB this inclusion is not related to the inclusion in A_n already noted). It is straightforward in this case to verify that the asymptotic growth rate is 4.

n	3	4	5	6	7	8	9	10
$\lvert C_n\rvert$	1	2	5	14	42	132	429	1430
$\lvert C_n\rvert/\lvert C_{n-1}\rvert$		2	2.5	2.8	3	3.14	3.25	3.33

This raises the question: Is there a limit rate in the Æ_n case?

8. On enumerable classes of strand diagrams and plabic graphs

Let Pb_n be the set of reduced plabic graphs [25, §11] of rank-n; and Po_n be the set of alternating strand diagrams as in [25, §14]. (See also Section 8.1 and (8.5).) Their relationship with A_n can be summarized as follows:

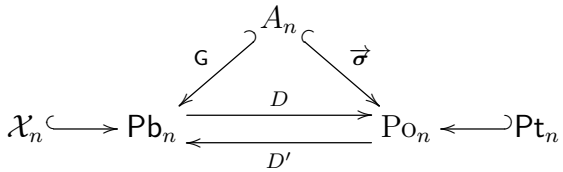

Here G is as in §1, $\overrightarrow{\boldsymbol{\sigma}}$ as in §2.1, and D, D' as in §8.2. In this section we apply Theorem 2.1 to corresponding subsets of plabic and strand diagrams. We define the sets $\mathcal{X}_n$ of *minimalist* strand diagrams, see Section 8.1; and Pt_n of *rhombic* (plabic) graphs, see (8.5). We will show that these sets are in bijection with A_n.

For the sake of brevity we refer to Postnikov's original paper for motivations behind the constructions of plabic and strand diagrams themselves. These are large and complex classes of objects, and canonical forms for them would be a useful tool. The rigid/canonical nature of A_n induces canonical forms for (the restricted cases of) the other constructions.

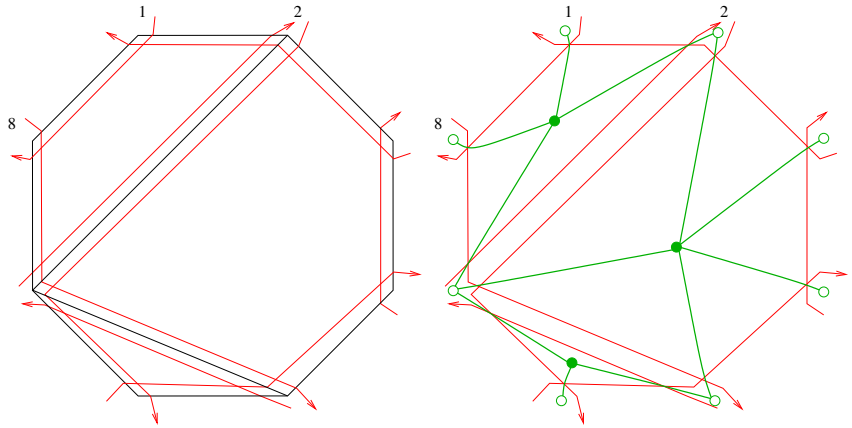

FIGURE 11. (a) A tiling T (black) with strand diagram $\overrightarrow{\boldsymbol{\sigma}}(T)$ of T; (b) the plabic graph $D'(\overrightarrow{\boldsymbol{\sigma}}(T))$ (green).

We start by characterizing the image of $\overrightarrow{\boldsymbol{\sigma}}$ in Theorem 8.4 as the set of minimalist strand diagram and hence show that $\overrightarrow{\boldsymbol{\sigma}}$ is injective. In Section 8.2 we recall Postnikov's bijections between alternating strand diagrams and plabic graphs. (An illustration of the connection between plabic and strand diagrams is given by Figure 11(b).) This allows us to characterize the image of G in Section 8.3 as the set of rhombic plabic graphs, Theorem 8.19. Finally we determine the images of flip equivalence in the two other realisations.

8.1. **On $\overrightarrow{\boldsymbol{\sigma}}$ and strand diagrams.** An *absolute strand diagram* on (S, M) is a Jordan diagram such that: (i) strands crossing a given strand must alternate in direction; (ii) if two strands cross twice such as to cut out a simple disk then the resultant loop is oriented; (iii) if a strand is self-crossing then no resultant loop is a simple disk; (iv) no strand is a closed loop cutting out a simple disk.

Note that this agrees with the ordinary definition of *alternating strand diagram* [25, 2] for S a simple disk. Here rank $n = |M_\partial| = |M|$.

For any directed planar graph we classify the faces as clockwise, counterclockwise, alternating or other.

(8.1) Let $\mathcal{X}_n$ be the subset of rank-n alternating strand diagrams whose faces are as follows: (i) n clockwise faces at the boundary, labelled $1, 2, \ldots, n$ going clockwise around the boundary; (ii) alternating faces with four sides; (iii) oriented faces in the interior that are counterclockwise and have at least 3 sides.

We call the elements of $\mathcal{X}_n$ *minimalist strand diagrams*. See Figure 12 for an example.

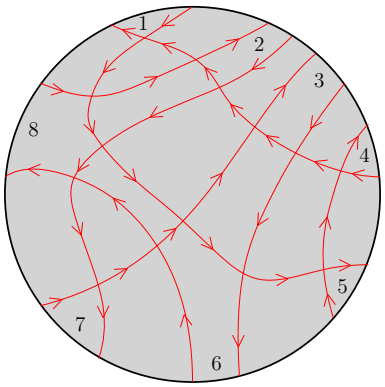

FIGURE 12. A Jordan diagram on the 8-gon that is an element of $\mathcal{X}_8$

(8.2) Note that an element of $\mathcal{X}_n$ (as every alternating strand diagram) has a chequerboard colouring of faces (see e.g. [25]). If a clockwise face is black (say) then all oriented faces are black and all alternating faces white. Also the faces around an alternating face alternate clockwise/counterclockwise.

(8.3) We define a 'shrink' map $\mathsf{f} : \mathcal{X}_n \to A_n$ as follows: Let $d \in \mathcal{X}_n$. Note from (8.2) that in d regarded as an isotopy class of concrete diagrams there are cases in which all the edges of clockwise faces are arbitrarily short. Thus the clockwise faces are arbitrarily small neighbourhoods of n points; and alternating edges have two short edges and two edges that pass between the clockwise faces (and hence are not short). The paths of non-short edges are not constrained by the 'shrinking' of the clockwise edges. Thus each pair may be brought close to each other, and hence form an arbitrarily narrow neighbourhood of a line between two of the n points. Since no two alternating faces intersect, these lines cannot cross, and so they form an element of A_n.

Theorem 8.4. *The map* $\mathsf{f} : \mathcal{X}_n \to A_n$ *is the inverse to a bijection* $\overrightarrow{\boldsymbol{\sigma}} : A_n \to \mathcal{X}_n$.

Proof. It will be clear that f makes sense on $\overrightarrow{\boldsymbol{\sigma}}(T)$ since it even makes sense tile by tile (cf. Fig.13). Indeed it recovers the tile, so f inverts $\overrightarrow{\boldsymbol{\sigma}}$. The other steps have a similar flavour. □

Remark. One can prove more generally, that $\overrightarrow{\boldsymbol{\sigma}}$ is injective on tilings of (S, M) and that the image of any tiling of (S, M) is an absolute strand diagram.

8.2. Maps D, D' between strand diagrams and plabic graphs.

(8.5) A *plabic graph* γ is a planar, disk-embedded undirected graph with two 'colours' of vertices/nodes, considered up to homotopy [25, Definition 11.5]. Vertices are allowed on the disk boundary. The rank of γ is the number of these 'tagged' vertices. In rank n they are labelled $\{1, 2, ..., n\}$ clockwise.

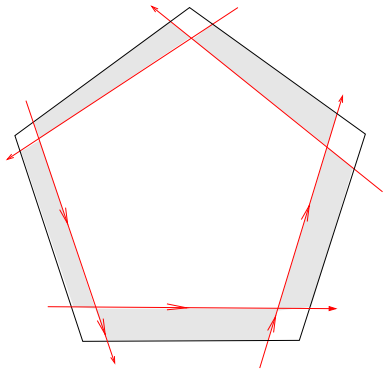

FIGURE 13. Strands partition a tile into vertex, edge and face parts.

Postnikov defines 'moves' on plabic graphs in [25, §12]:

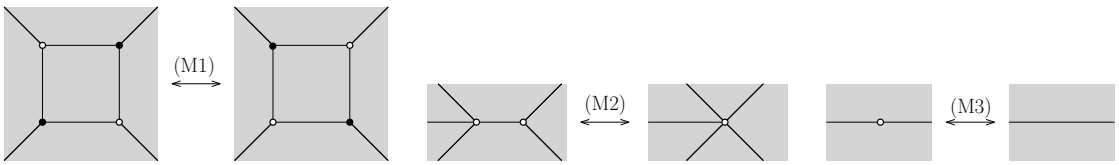

with M2-3 also for black nodes. In M2 any number of incoming edges is allowed. Postnikov also defines reductions on plabic graphs:

and similarly with colours reversed. The *move-equivalence class* of γ is its orbit under (M1-3). A plabic graph of rank n is *reduced* if it has no connected component without boundary vertices; and if there is no graph in its move-equivalence class to which (R1) or (R2) can be applied. See [25, §12] for details. We write Pb_n for the set of reduced plabic graphs of rank n.

Recall the map G on A_n to plabic graphs from §1. If T is a tiling of an n-gon, we draw a white node at each vertex of the polygon and a black node in each tile, connecting the latter by edges with the white nodes at the vertices of the tile. One can see that the graph produced has no parallel bicoloured edges and no internal leaves with bicoloured edges. Thus $\mathsf{G} : A_n \to \mathsf{Pb}_n$.

Postnikov's plabic *networks* are generalisations of the above including face weights. Here it will be convenient to consider another kind of generalisation.

(8.6) For any planar graph L there is a *medial graph* $\mathsf{m}(L)$ (see e.g. [4, §12.3]), which is a planar graph distinct from but overlaying L. We obtain $\mathsf{m}(L)$ by drawing

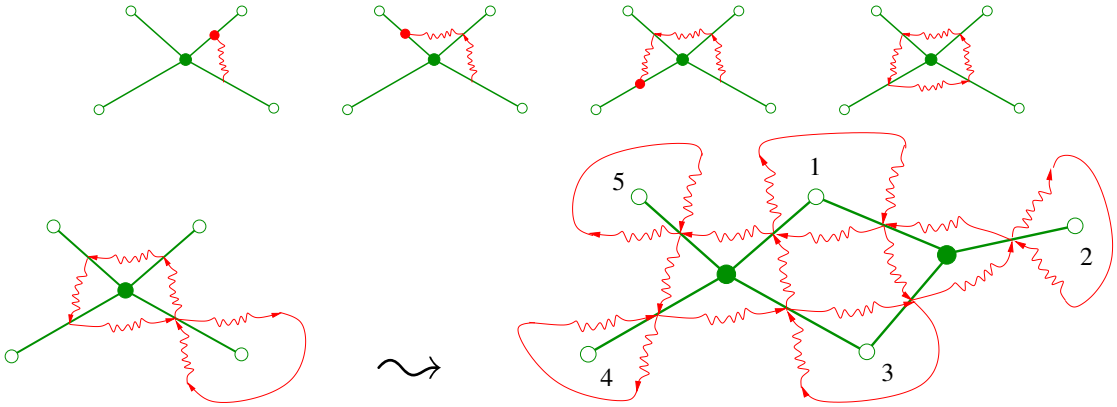

FIGURE 14. Constructing the D-map

a vertex $\mathsf{m}(e)$ on each edge e of L, then whenever edges e, e' of L are incident at v and bound the same face we draw an edge $\mathsf{m}(e)$-$\mathsf{m}(e')$.

(8.7) For $\mathsf{m}(L)$ we note the following. (1) $\mathsf{m}(L)$ has a polygonal face p_v around each vertex v of L. (2) Monogon and digon faces are allowed — see Figure 14 (so edges may not be straight). (3) The faces of $\mathsf{m}(L)$ are of two types: containing a vertex of L, or not. Given an asignment of a colour (black/white) to each vertex of L then we get a digraph $\overrightarrow{\mathsf{m}}(L)$ by asigning an orientation to each polynomial face: counterclockwise if v is black and clockwise otherwise. (4) If L is bipartite and indeed 2-coloured then for this asignment the orientations in $\overrightarrow{\mathsf{m}}(L)$ have the property that we may reinterpret the collection of meeting oriented polygons as a collection of crossing oriented strands, denoted D_L.

(8.8) Suppose L has some labelled exterior vertices. A 'half-edge' or 'tag' may be attached to any such vertex v (specifically one usually thinks of L bounded in a disk in the plane, and the tag as an edge passing out through the boundary) whereupon there is a medial vertex $\mathsf{m}(v)$ on the half-edge, and the (exterior) medial edge around v becomes two segments incident at $\mathsf{m}(v)$. In this case, if v is labelled in L then we say that $\mathsf{m}(v)$ inherits this label in $\mathsf{m}(L)$.

(8.9) Noting (8.7) and (8.8), the map

$$D : \mathsf{Pb}_n \to \mathrm{Po}_n$$

may be defined by $D(L) = D_L$.

(8.10) A *fully reduced* plabic graph is a reduced plabic graph without non-boundary leaves; and without unicolored edges. In particular it is a connected 2-coloured planar graph. Write Pf_n for the set of fully reduced plabic graphs of rank n.

Postnikov's Corollary 14.2(1) can now be summarized as: $L \mapsto D_L$ restricts to a bijection $D : \mathsf{Pf}_n \to \mathrm{Po}_n$.

(8.11) Postnikov gives a map

$$D' : \mathrm{Po}_n \to \mathsf{Pf}_n$$

as follows, that inverts D. Let d be an alternating strand diagram. Then $D'(d) = \gamma_d$ is the plabic graph we obtain by drawing a white vertex in each clockwise oriented face and a black vertex in each counterclockwise face. Two vertices are connected by an edge if and only if their faces are opposite each other at the crossing point of a pair of crossing strands. (Example: Figure 11.)

8.3. **Properties of the map G.**

We note that G is the composition $D' \circ \overrightarrow{\boldsymbol{\sigma}}$. Since D' is a bijection and $\overrightarrow{\boldsymbol{\sigma}}$ is injective (Theorem 8.4), G is injective. In this section, we give an intrinsic characterization of the image of G.

(8.12) Let u and v be two black nodes in $\gamma \in \mathsf{Pf}_n$ that are on a common quadrilateral. If u has degree $r+2$ and is incident with $r \geq 1$ leaves, we say that γ has an *r-bouquet* at u or a *bouquet* at u. The subgraph on the quadrilateral and on the r leaves is the bouquet at u.

The first figure below is a bouquet at u with 4 leaves. The second figure shows two (non-disjoint) bouquets, one at u and one at v. The second graph has two bouquets. It satisfies the conditions for Pt_n of Definition 8.13.

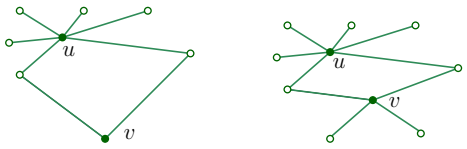

Definition 8.13. The set Pt_n of *rhombic graphs* is the set of connected fully reduced plabic graphs γ in Pf_n containing at least one black node and such that
(a) the tagged nodes (in the sense of (8.5)) are white and all other nodes are black,
(b) every black node has degree ≥ 3,
(c) every closed face is a quadrilateral,
(d) in the fan of edges coming out of a white node every adjacent pair is part of a quadrilateral.

(8.14) We observe that conditions (a) and (b) imply: (e) Two faces of a rhombic graph share at most one edge.

For $n = 3, 4, 5$, Pt_n has 1,3,11 elements respectively, cf. Figure 15.

Lemma 8.15. *If $\gamma \in \mathsf{Pt}_n$, γ not a star, then γ has at least two bouquets.*

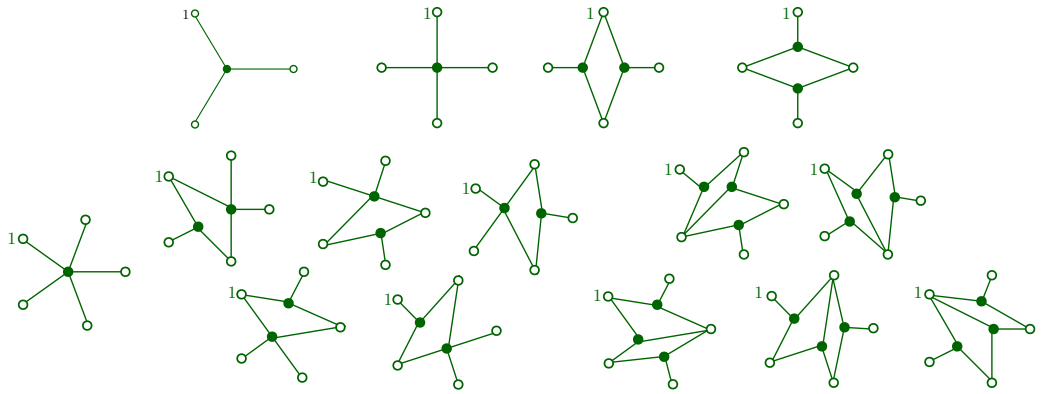

FIGURE 15. Pt_n in ranks $n = 3, 4, 5$

Proof. Forget the leaves for a moment, so we have graph of quadrilaterals. Now consider the exterior 'face' subgraph - a 2-coloured loop. We see (e.g. by induction on number of faces, using (8.14)) that this must have at least 2 black corners (black nodes touching only 1 quadrilateral). □

We note that $\mathsf{G}(A_n) \subseteq \mathsf{Pt}_n$. Our next goal is to get an inverse to the map G, going from rhombic graphs to tilings. One ingredient is the following lemma which says that if we split an element of Pt_n at a bouquet at node u, we obtain a star graph and an element γ_u of Pt_n.

(8.16) Let γ be a plabic graph containing a bouquet at vertex u, with u of degree $r+2$. Define γ_u as the full subgraph on the vertex set excluding u and its leaves. We denote by γ_s the full subgraph on u and all white nodes incident with u.

For example here γ_s is the upper graph on the right and γ_u is the lower graph on the right.

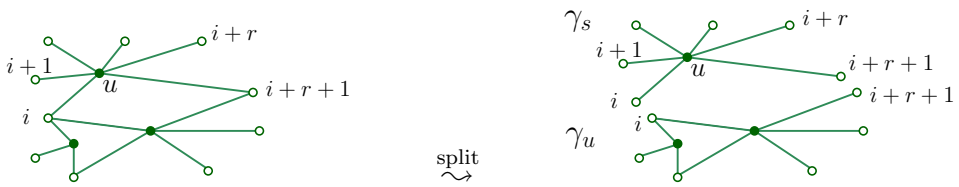

Lemma 8.17. *Let $\gamma \in \mathsf{Pt}_n$, γ not a star. If γ has a bouquet at u then $\gamma_u \in \mathsf{Pt}_n$.*

Proof. Note that γ_u inherits (a) and (b) of Definition 8.13 from γ. Denote the second black node of the bouquet at u by v. When splitting, the quadrilateral face involving u and v becomes a boundary face of γ_u. All other faces of γ_u are faces of γ. So (c) also holds.

It remains to see that (d) holds for γ_u. The only vertices to check are $i+1$ and $i+r+1$. In γ, every adjacent pair of edges at $i+1$ (or at $i+r+1$ respectively)

are part of a quadrilateral. When going to γ_u, one extremal edge of the fan is removed, so the remaining edges still satisfy (d). □

(8.18) Let $\gamma \in \mathsf{Pt}_n$. Consider the set

$$\{[i,j] \mid i \text{ and } j \text{ are white nodes in a quadrilateral of } \gamma\}$$

Note (by 8.13(a) and the construction) that this forms a collection of pairwise non-crossing diagonals of an n-gon. We denote this tiling $T = \mathsf{G}'(\gamma)$.

Theorem 8.19. *The map G' is the inverse to a bijection G: $A_n \to \mathsf{Pt}_n$.*

Proof. We will show that $\mathsf{G}\mathsf{G}'(\gamma) = \gamma$ for every $\gamma \in \mathsf{Pt}_n$.

We use induction on n. If $|\gamma| = 3$, by Definition 8.13, γ does not contain any quadrilaterals, hence is a star, and $\mathsf{G}'(\gamma)$ is the untile T of a triangle, with $G(T) = \gamma$. So assume that the claim is true for Pt_{n-1}. Take $\gamma \in \mathsf{Pt}_n$. If γ is a star, $T = \mathsf{G}'(\gamma)$ is the untile of the n-gon and $\mathsf{G}(T) = \gamma$. So assume γ is not a star. By Lemma 8.15, it then contains at least two bouquets, say an r-bouquet for some $1 \leq r < n-2$.

We split γ at the bouquet and obtain a star γ_s and the graph γ_u. Let the white nodes of this star be $i, i+1, \ldots, i+r+1$ (reducing mod n). Then the white nodes of γ_u are $i+r+1, i+r+2, \ldots, i$ (reducing mod n). Graphs γ_s and γ_u are elements of Pt_{r+2} (with $r+2 < n$) and Pt_{n-r} respectively by Lemma 8.17. So by induction for the tilings $T_s = \mathsf{G}'(\gamma_s)$ and $T_u = \mathsf{G}'(\gamma_u)$ of polygons we have $\mathsf{G}(T_s) = \gamma_s$ and $\mathsf{G}(T_u) = \gamma_u$.

Tiling T_s is the untile of the polygon P_s on the vertices $i, i+1, \ldots, i+r+1$; $T_u = \mathsf{G}'(\gamma_u)$ a tiling of the polygon P_u on the vertices $i+r+1, i+r+2, \ldots, i$.

We glue the two polygons P_s and P_u along the boundary edges $[i+r+1, i]$ and $[i, i+r+1]$ to obtain an n-gon P with vertices $1, 2, \ldots, n$ and tiling T given by the union of the diagonals of T_s, T_u and diagonal $[i, i+r+1]$.

Since T contains a diagonal exactly for every quadrilateral in γ, $T = \mathsf{G}'(\gamma)$. By construction, $\mathsf{G}(T) = \gamma$. □

8.4. Pt_n and equivalence classes under moves.

(8.20) We define 'moves' $\rho_\diamond$ on elements of Pt_n as in Fig.16 (these moves are a particular combination of M1 and M2 from §8.2).

Lemma 8.21. *Under the bijection $\mathsf{G}' : \mathsf{Pt}_n \to A_n$, a move $\rho_\diamond$ corresponds to a flip in a tiling.*

Proof. Consider $\gamma \in \mathsf{Pt}_n$, let $T = \mathsf{G}'(\gamma)$. Any quadrilateral $\diamond$ in γ corresponds to a diagonal $[p_1, p_3]$ in T. Now assume that two black nodes u_1, u_2 of the quadrilateral $\diamond$ have degree three and let p_2, p_4 be the other two white nodes adjacent to the black nodes of $\diamond$. Then the four full subgraphs p_i, u_j, p_{i+1} (with i, j appropriate) of γ are either boundary paths or part of quadrilaterals. In the former case, the image of γ under G' has a boundary segment $[p_i, p_{i+1}]$; in the latter case, it has a diagonal

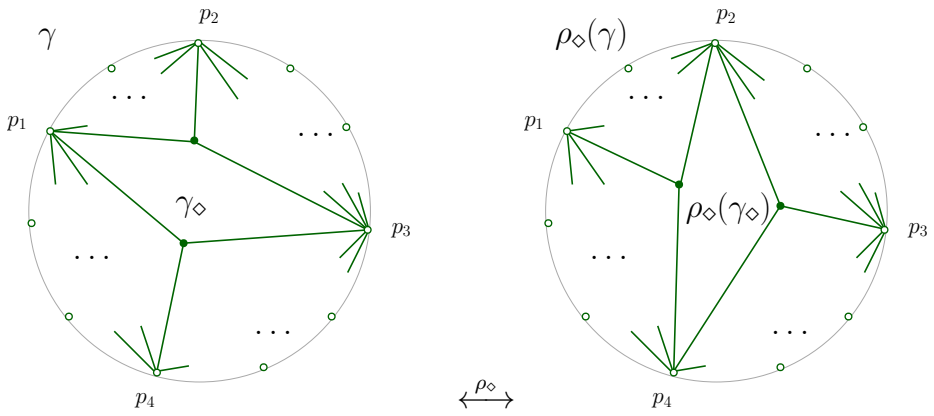

FIGURE 16. Move $\rho_\diamond$ in Pt_n

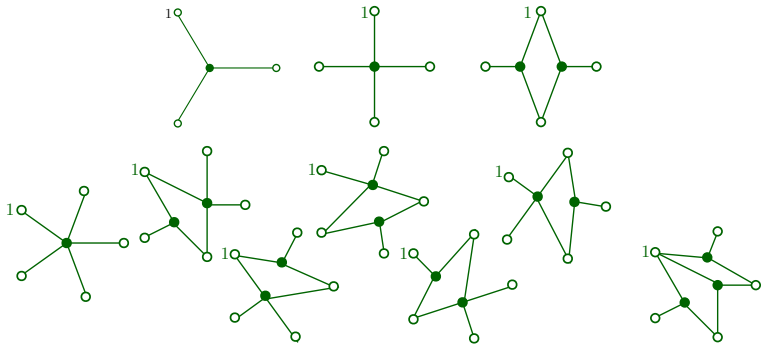

FIGURE 17. Classes $\mathsf{Pt}_n/\sim$ in ranks $n = 3, 4, 5$

$[p_i, p_{i+1}]$. In any case, T contains a triangulated quadrilateral p_1, p_2, p_3, p_4 with diagonal $[p_1, p_3]$ and the move $\rho_\diamond$ corresponds to the exchange $[p_1, p_3] \longleftrightarrow [p_2, p_4]$ in T. □

Given Lemma 8.21 we can then define move-$\rho_\diamond$ equivalence classes $\mathsf{Pt}_n/\!\sim$ on Pt_n. Furthermore, the number of equivalence classes are the same as $|Æ_n|$.

For $n = 3, 4, 5$, one can readily confirm $1, 2, 7$ classes respectively using Figure 17. (Although this does not provide any obvious new method to compute in higher ranks, cf. §7.)

(8.22) On strand diagrams, flip corresponds to a combination of moves from Figure 18 (recalled from [25, §14]) — the combination given in §2.1.

(8.23) There are many beautiful set sequences in the little Schröder combinatoric [30] (A_n is a standard one, to which we have now added Pt_n and $\mathcal{X}_n$). It is one nice problem for future consideration to recast flip equivalence into cases such as Schröder's original bracket sequences (the set Ω_n is the set of properly nested

FIGURE 18. Postnikov's moves of alternating strand diagrams

bracketings on a word of length $n-1$, where there is always an (undrawn) outer bracketing and otherwise each bracket pair must contain at least two symbols — the bijection with A_n is elementary via rooted versions of the dual trees of §3). As a taste of this game, the first few in this case are as follows: $\Omega_3 = \{ab\}$, $\Omega_4 = \{abc, (ab)c, a(bc)\}$, and in A-complex form

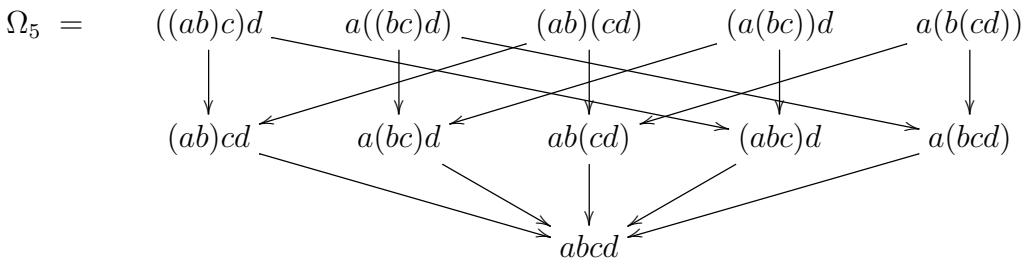

Here flip equivalence collapses the entire first row to a point.

Acknowledgements. We thank Henning H. Andersen, Aslak B. Buan and Walter Mazorchuk and the Mittag-Leffler Institute for inviting us to the 2015 Semester on Representation Theory, where this work was started. We thank Robert Marsh and Hannah Vogel for useful comments on the manuscript. PM would like to thank EPSRC for partial funding under the grant EP/I038683/1 "Algebraic, Geometric and Physical underpinnings of Topological Quantum Computation". KB would like to thank FWF for partial funding under projects P25141-N26, P 25647-N26 and W1230.

REFERENCES

1. B. Balsam and A. Kirillov Jr., *Turaev-Viro invariants as an extended TQFT*, arxiv (1004.1533v3).
2. K. Baur, A. King, and R.J. Marsh, *Dimer models and cluster categories for Grassmannians*, preprint (1309.6524v1.pdf).
3. K. Baur and P.P. Martin, *GAP macros refining the Fuss–Euler combinatoric*, GAP code available at http://www1.maths.leeds.ac.uk/∼ppmartin/GRAD/NOTES/COMBINATORICS/GRaZ.g (2015).
4. R. Baxter, *Exactly solved models in statistical mechanics*, Academic Press, 1982.
5. C. Bessenrodt, *Conway-Coxeter friezes and beyond: Polynomially weighted walks around dissected polygons and generalized frieze patterns*, J. Algebra **442** (2015), 80–103.

6. A. I. Bobenko and B. A. Springborn, *A discrete Laplace-Beltrami operator for simplicial surfaces*, Discrete Comput. Geom. **38** (2007), 740756.
7. J. A. Bondy and U. S. R. Murty, *Graph theory*, GTM244, Springer, 2007.
8. T. Brüstle and J. Zhang, *On the cluster category of a marked surface without punctures*, Algebra Number Theory **5** (2011), no. 4, 529–566.
9. V. Buchstaber, *Fullerenes and polygonal partitions of surfaces*, Workshop on Analysis, Geometry and Probability, Ulm (2015), (online, workshop September-October 2015).
10. V. Fock and A. Goncharov, *Dual Teichmüller and lamination spaces*, Handbook of Teichmüller theory. Vol. I (A. Papadopoulos, ed.), Eur. Math. Soc., Zürich, 2007, pp. 647–684.
11. S. Fomin, M. Shapiro, and D. Thurston, *Cluster algebras and triangulated surfaces. Part I: Cluster complexes*, Acta Math. (2008), no. 201, 83–146.
12. The GAP Group, *GAP – Groups, Algorithms, and Programming, Version 4.7.9*, 2015.
13. J.L. Harer, *Stability of the homology of the mapping class groups of orientable surfaces*, Annals of Math. **121** (1985), 215–249.
14. A. Hatcher, *On triangulations of surfaces*, Topology Appl., (1991), no. 40, 189–194.
15. N.V. Ivanov, *Mapping class groups*, Handbook of geometric topology (R.J. Daverman and R.B. Sher, eds.), North-Holland, Amsterdam, 2002, pp. 523–633.
16. A. Kirillov Jr., *On piecewise linear cell decompositions*, Algebr. Geom. Topol. **12** (2012), no. 1, 95–108.
17. Z. Kadar, P. Martin, and S. Yu, *On geometrically defined extensions of the Temperley-Lieb category in the Brauer category*, arxiv (2014), http://arxiv.org/abs/1401.1774.
18. A. Kitaev, *Fault-tolerant quantum computation by anyons*, Ann. Physics (2005).
19. D. E. Knuth, *Sorting and searching*, 2 ed., The Art of Computer Programming, vol. 3, Addison Wesley, 1998.
20. S. K. Lando and A. K. Zvonkin, *Graphs on surfaces*, Springer, 2004.
21. R. Marsh and P. Martin, *Pascal arrays: counting Catalan sets*, arxiv (2006), http://arxiv.org/pdf/math/0612572v1.pdf.
22. E.E. Moise, *Geometric topology in dimensions 2 and 3*, Graduate Texts in Mathematics 47, Springer-Verlag, New York, 1977.
23. D. Mugnolo, *Semigroup methods for evolution equations on networks*, Springer, 2014.
24. T.K. Petersen, P. Pylyavskyy, and B. Rhoades, *Promotion and cyclic sieving via webs*, J. Algebraic Combin. **30** (2009), no. 1, 19–41.
25. A. Postnikov, *Total positivity, Grassmannians, and networks*, preprint (arXiv:math/0609764).
26. J. Propp, *The combinatorics of frieze patterns and Markoff numbers*, http://arxiv.org/pdf/math/0511633v4.pdf (2005).
27. J.H. Przytycki and A.S. Sikora, *Polygon dissections and Euler, Fuss, Kirkman and Cayley numbers*, J. Combin. Theory Ser. A **92** (2000), no. 1, 68–76, arXiv:math/9811086v1.
28. N. Reading, *Clusters, Coxeter-sortable elements and non-crossing partitions*, Trans. AMS (2007), (See also: Catalan, 321-perm, talk online.).
29. J. Scott, *Grassmannians and cluster algebras*, Proc. London Math. Soc. **92** (2006), no. 2, 345–380.
30. R. P. Stanley, *Enumerative combinatorics*, Cambridge, 1997.

* Department of Mathematics and scientific computing, University of Graz, Nawi Graz, 8010 Graz, Austria

** Department of Pure Mathematics, University of Leeds, Leeds LS2 9JT, UK